A geodynamic model linking Cretaceous orogeny, arc migration, foreland dynamic subsidence and marine ingression in southern South America

Guido M. Gianni, Federico M. Dávila, Andrés Echaurren, Lucas Fennell, Jonathan Tobal, Cesar Navarrete, Paulo Quezada, Andrés Folguera, Mario Giménez

PII: S0012-8252(18)30166-1
DOI: doi:10.1016/j.earscirev.2018.06.016
Reference: EARTH 2655

To appear in: *Earth-Science Reviews*

Received date: 15 March 2018
Revised date: 8 May 2018
Accepted date: 25 June 2018

Please cite this article as: Guido M. Gianni, Federico M. Dávila, Andrés Echaurren, Lucas Fennell, Jonathan Tobal, Cesar Navarrete, Paulo Quezada, Andrés Folguera, Mario Giménez , A geodynamic model linking Cretaceous orogeny, arc migration, foreland dynamic subsidence and marine ingression in southern South America. Earth (2018), doi:10.1016/j.earscirev.2018.06.016

A geodynamic model linking Cretaceous orogeny, arc migration, foreland dynamic subsidence and marine ingression in southern South America

Guido M. Gianni[1], Federico M. Dávila[2], Andrés Echaurren[3], Lucas Fennell[3], Jonathan Tobal[3], Cesar Navarrete[4], Paulo Quezada[5], Andrés Folguera [3], Mario Giménez[1].

1. IGSV. Instituto Geofísico Sismológico Ing. F. Volponi. Universidad de Nacional San Juan, San Juan, Argentina
2. CICTERRA-CONICET and Universidad Nacional de Córdoba, Córdoba, Argentina
3. IDEAN. Instituto de Estudios Andinos Don Pablo Groeber. Universidad de Buenos Aires-Conicet, Capital, Argentina
4. Universidad Juan Don Bosco, Comodoro Rivadavia, Argentina
5. Universidad Andrés Bello, Departamento de Geología, Concepción, Chile

Abstract

This study synthesizes the tectonomagmatic evolution of the Andes between 35°30'S to 48°S with the aim to spotlight early contractional phases on Andean orogenic building and to analyze their potential driving processes. We examine early tectonic stages of the different fold-thrust belts that compose this Andean segment. Additionally, we analyzed the spatio-temporal magmatic arc evolution as a proxy of dynamic changes in Andean subduction during critical tectonic stages of orogenic construction. This revision proposes a hypothesis related the existence of a continuous large-scale flat subduction setting in Cretaceous times with a similar size to the present-largest flat-slab setting on earth. This potential process would have initiated diachronically in the late Early Cretaceous and achieved full development in Late Cretaceous to earliest Paleocene times, constructing a series of fold-thrust belts on the retro-arc zone from 35°30'S to 48°S. Moreover, we assess major paleogeographic changes that took place during flat-slab full development in Maastrichtian-Danian times. At this moment, an enigmatic Atlantic-derived marine flooding covered the Patagonian foreland reaching as far as the Andean foothills. Based on flexural and dynamic topography analyses, we suggest that focused dynamic subsidence at the edge of the flat-slab may explain sudden marine ingression previously linked to continental tilting and orogenic loading during a high sea level global stage. Finally, flat-subduction destabilization could have triggered massive outpouring of synextensional intraplate volcanic rocks in southern South America and the arc retraction in late Paleogene to early Neogene times.

Keywords: Andes, broken foreland, flat-slab, dynamic subsidence, marine transgression.

1. Introduction

In spite of many years of scientific research in the Andes, type locality of subduction orogenesis, several aspects regarding to their evolution, deformational mechanisms, and uplift timing remain unsolved. Even though most recent tectonic research is increasingly supporting pre-Cenozoic initial growth of the Andean orogen (e.g., Dalziel et al., 1974; Mégard, 1984; Wilson, 1991; Fildani et al., 2003; Folguera and Iannizzotto, 2004; Mpodozis et al., 2005; Arriagada et al., 2006; Jaimes and de Freitas, 2006; Martin-Gombojav and Winkler, 2008; Tunik et al., 2010, Horton et al. 2001; 2017, 2018 among others), contraction achieved during these stages is still underestimated in recent works assessing Andean evolution (e.g., Oncken et al., 2006; Husson et al., 2008; Barnes and Elhers, 2009; Maloney et al., 2013; Faccena et al., 2013; Armijo et al., 2015). Deciphering early Andean stages is of paramount importance for a better understanding of the relation among tectonic processes, topographic evolution and climate changes in South America (e.g., Poulsen et al., 2010; Garzione et al., 2006). Additionally, it would help to constrain studies assessing spatial and temporal patterns in hydrology and ecology (e.g., Hoorn et al., 2010; Mulch et al., 2010; Rorhman et al., 2014) which have major implications on geogenomics and speciation (e.g., Baker et al., 2014).

Some outstanding examples of the contribution of pre-Cenozoic stages to Andean orogenic building come from most recent studies carried on fold-thrust belts composing the Southern Central and Southern Andes. In this contribution, we synthesize the latest geologic advances of the Malargüe, Chos Malal, Agrio, Aluminé and North Patagonian fold-thrust belts, as well as in the Patagonian broken foreland (Fig. 1), to highlight the role of early orogenic stages. Additionally, we review the time-space arc behavior between 35°30'S to 48°S, which is helpful to gain insights into several potential geodynamic processes in subduction margins such as increase/decrease in plate coupling manifested on subduction erosion/accretion (Von Huene and Scholl, 1991; Kay et al., 2005), changes in convergence rates (Molnar et al., 1979), crustal thickening (Karlstrom et al., 2014) and variations in slab dip (Coney and Reynolds, 1977). Then, we discuss the potential geodynamic mechanisms behind early mountain building stages and changes in arc dynamics. Finally, we carried a new flexural study and a dynamic topography analysis adopting the model of Eakin et al. (2014), to assess the origin of paleogeographic modifications linked to an enigmatic marine ingression in latest Cretaceous to Paleogene times.

2. Cretaceous contractional deformation stages.

The following subsections are an update of geological studies from extensive research done in the last decade in the Andes of southern South America (Fig. 1b). Particularly, we focus on a segment extending ~1400 km from the 35°30' to 48°S that encompasses the Malargüe, Chos Malal, Agrio, Aluminé and North Patagonian fold-thrust belts; and the Patagonian broken foreland in the intraplate sector (Fig. 1b).

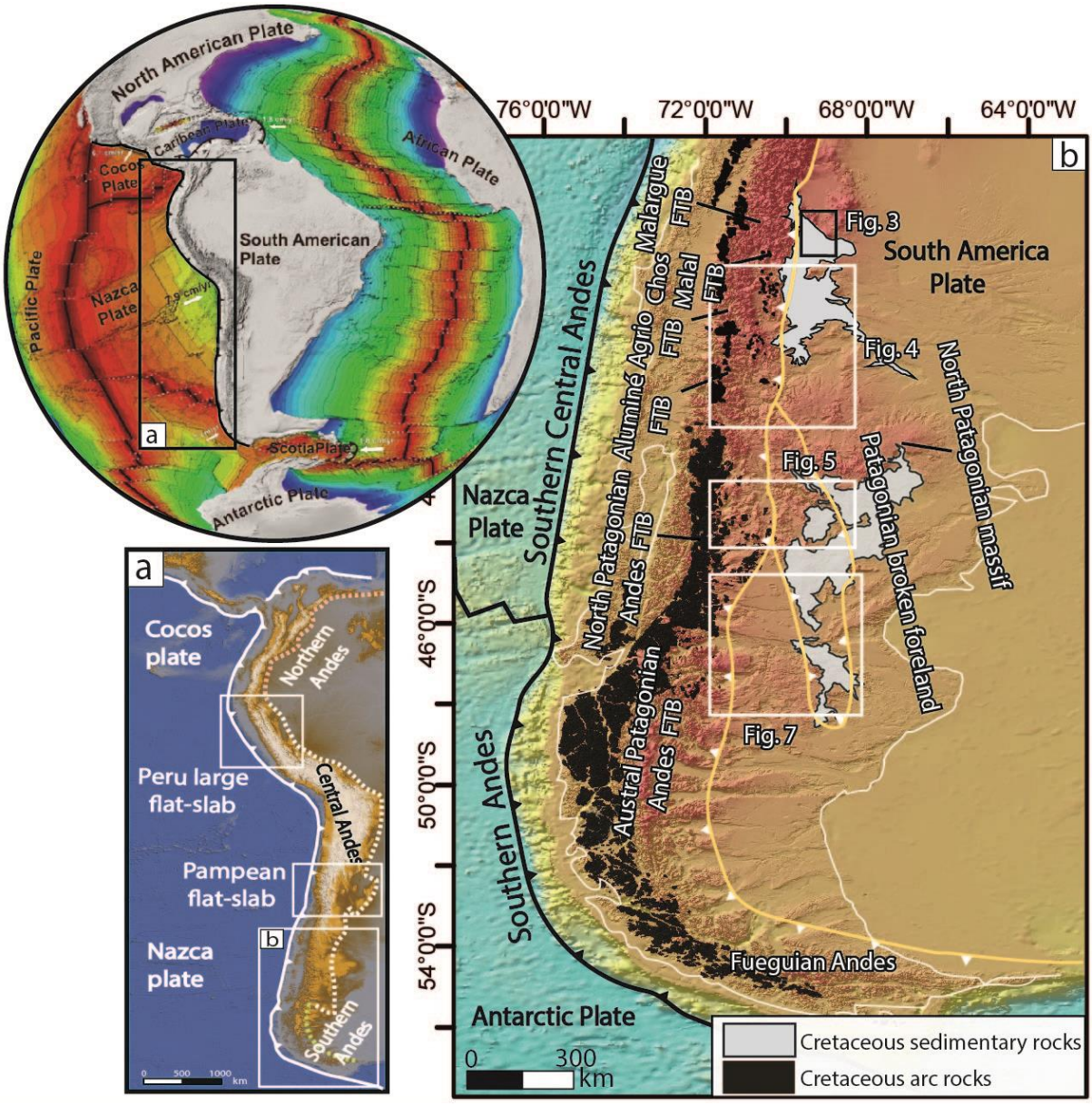

Fig. 1. a) DEM showing the configuration of the Andes and location of the study area. b) Image depicting the Southern Central and Southern Andes with respective fold-thrust belts where Cretaceous orogeny has been documented. FTB: fold-thrust belt.

2.1. Late Early Cretaceous deformation in the Malargüe fold-thrust belt

The Malargüe fold-thrust belt has been object of many classic studies developed in the last decades of the 20th century due to its importance in the oil industry (Legarreta and Gulisano, 1989; Uliana et al., 1989; Gulisano and Gutierrez Pliemling, 1994; Manceda and Figueroa, 1995; Vergani et al., 1995, among others). Since its definition by Kozlowski et al. (1993), there has been a general acceptance that its main contractional phase took place during Miocene times (Silvestro et al., 2005; Giambiagi et al., 2008; Silvestro and Atencio, 2009; Turienzo et al., 2012). However, initial contraction in this belt began as early as Late Cretaceous (e.g., Groeber, 1946).

During the 70's to early 80's, studies mostly focused in the Late Cretaceous red beds of the Neuquén Group concluded that these deposits represented a foreland basin related to the Late Cretaceous orogen (Cazau and Uliana, 1973; Ramos, 1999 and references therein; for a summary, see Garrido 2010) (Fig. 2). Since then, numerous studies in the Malargüe fold-thrust belt have arrived at similar conclusions based on sedimentological, magmatic and seismic evidence (Galarza et al., 2009; Orts et al., 2012a; Spagnuolo et al., 2012; Mescua et al., 2013; Sánchez and Asurmendi, 2014). Direct evidence of Cretaceous tectonic activity in individual structures of this belt has been recently described by Fennell et al. (2015). These authors identified contractional growth strata in outcrops of the Neuquén Group in main structures of the Malargüe fold-thrust belt between 35º30' and 37ºS (Fig. 3a,b,c). Through the identification of growth strata, Fennell et al. (2015) defined the Late Cretaceous orogenic front, the general morphology of the orogen and the sediment paleoflow between 35º30' and 37ºS.

In order to represent the Late Cretaceous orogen, two schematic structural cross-sections were performed by Fennell et al. (2015) (location in Fig. 3a). In the northern section (Fig. 3d), the Sierra Azul and the Ranquil Co. anticlines were uplifted in Late Cretaceous times, defining a broad intermontane basin between them, where the Río Grande flows nowadays. The western structure had its core exhumed and was actively eroded, while the eastern structure was located in the wedge-top area, where both deformation and sedimentation processes took place. The Sierra Azul anticline was also the source of the sediments hosted in the Portezuelos Colorados syncline, an active structure during Late Cretaceous times (Orts et al., 2012a). In the southern section (Fig. 3e), the Sierra de Cara Cura was uplifted, defining an intermontane basin between this structure and the Puntilla de Huincán, which was interpreted by Galarza et al. (2009) as active at this time based on the observation of significant thickness changes in the Neuquén Group. This intermontane basin was fed by both, the Sierra de Cara Cura and Puntilla de Huincán structures. Towards the east, in the Bordo Alto del Payún, Sánchez and

Asurmendi (2014) documented the presence of a Late Cretaceous flexural depocenter that received sediments from the Sierra de Cara Cura at that time (Fig. 3e).

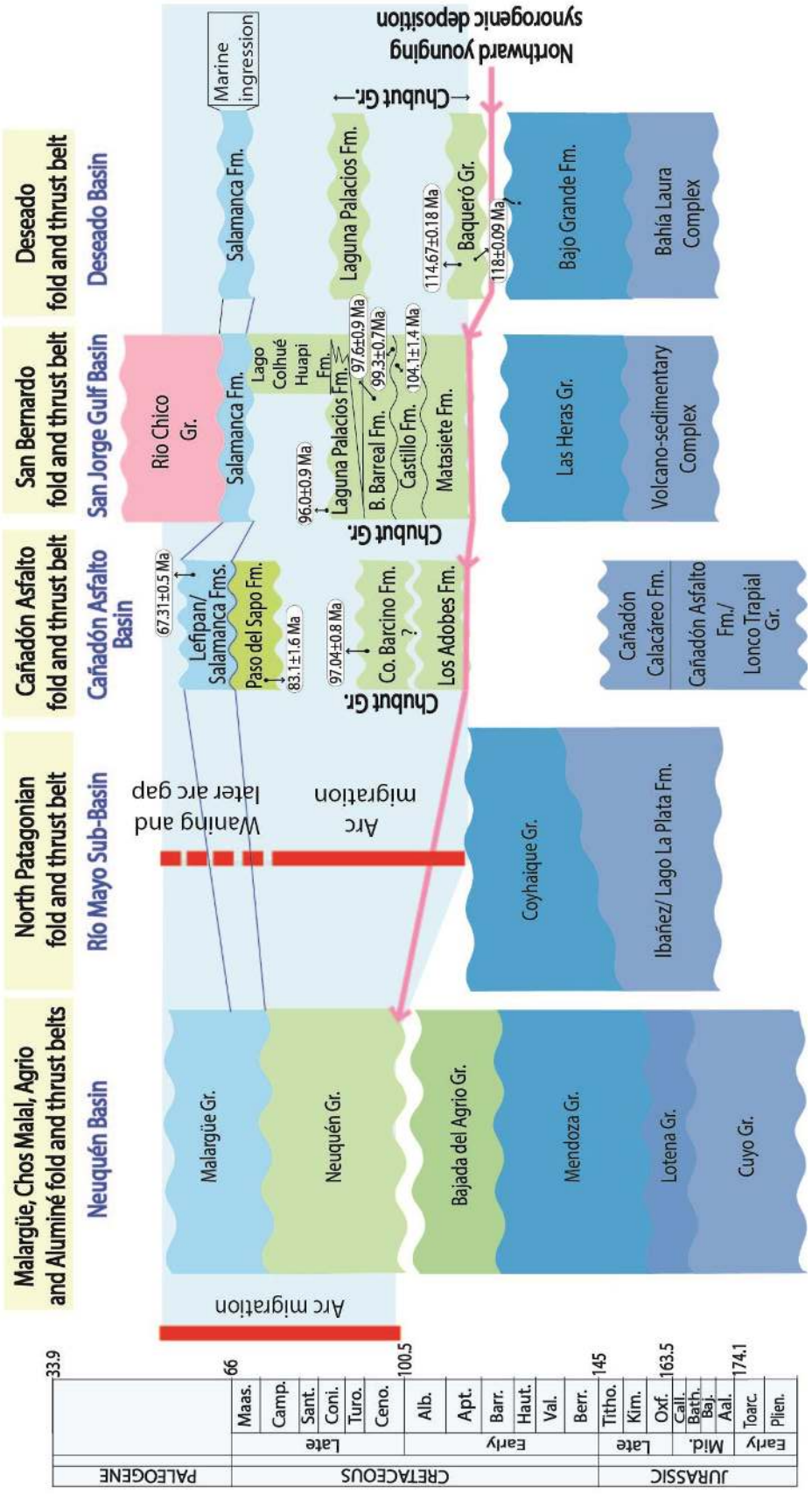

Fig. 2. Jurassic to Paleogene basin stratigraphy involved in the analyzed fold-thrust belts. Based on García Morabito and Ramos, (2012), Fennell et al. (2015), Gianni et al. (2015a) and Echaurren et al. (2016a).

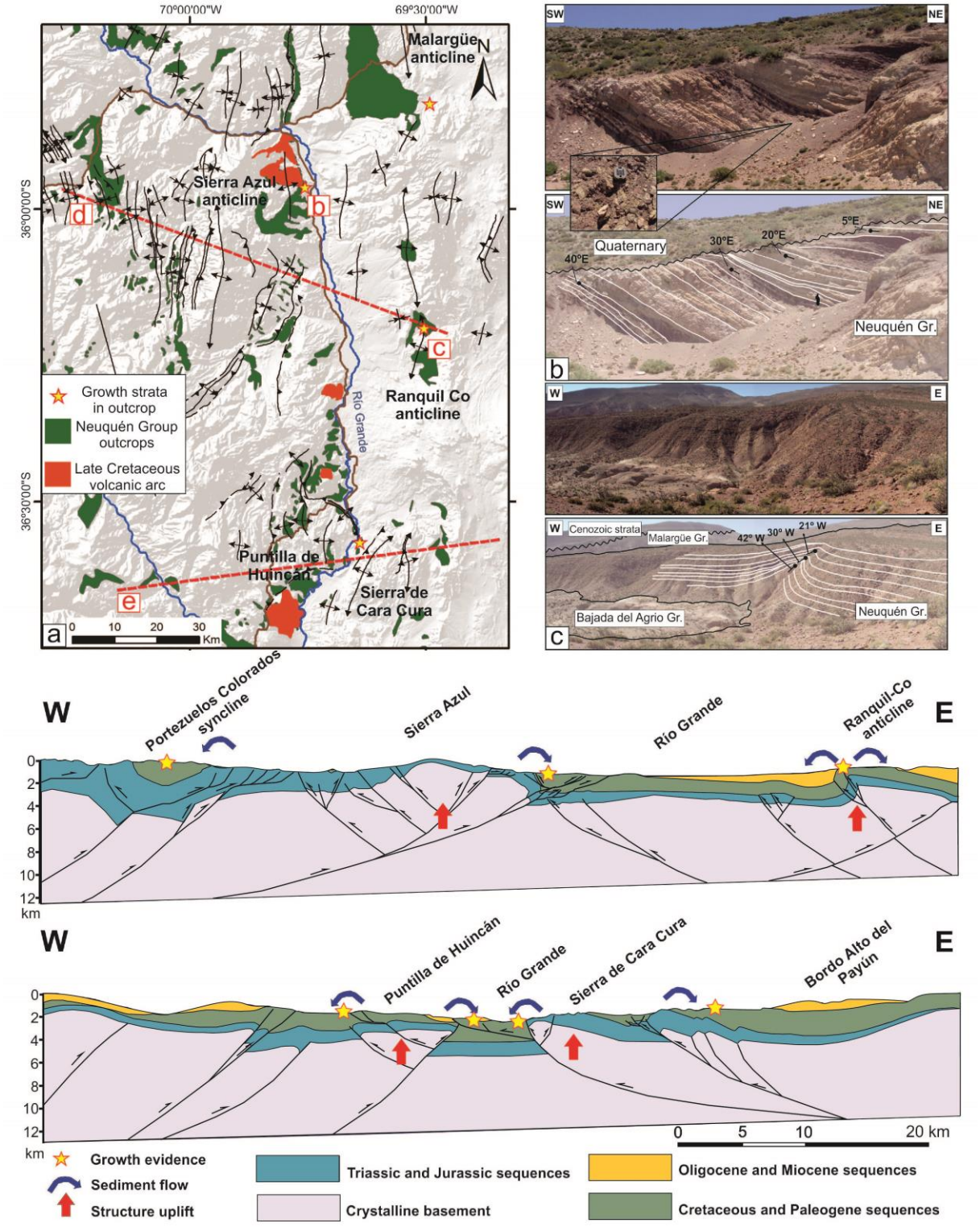

Fig. 3. a) DEM of the study area in the Malargue FTB showing the location of the identified growth strata in the Neuquén Group associated with the initial uplift of main anticlines in the

area. b) Growth evidences in strata of the Neuquén Group, located in the eastern-frontal limb of the Sierra Azul anticline. In the inset, angular intraclasts of the Neuquén Group can be observed. c) Growth strata in the Ranquil Co anticline, where a maximum depositional age of 100 Ma for the Neuquén Group was obtained through U-Pb detrital zircon ages. d) and e) Schematic cross-sections reflecting the dimensions of the Late Cretaceous orogen, along with the Late Cretaceous structures identified through field growth-strata evidences and other bibliographic mentions. Initial exhumation of the structures (red arrows) is constrained by apatite fission track analysis performed by Folguera et al. (2015). See Fig. 1a for location of cross-sections. Fig. modified from Fennell et al. (2015).

According to Fennell et al.(2015), the Late Cretaceous orogenic front was set 400-500 km east from the present trench, roughly reaching 69º30'W. Through U-Pb dating of detrital zircons in the Neuquén Group, the latter authors constrained the onset of deformation in this belt in ~100 Ma. To the North, between 35º30' and 33ºS, Mescua et al. (2013) had defined the Late Cretaceous orogenic front near the present international limit with Chile. Nevertheless, recent studies from the oil industry based on 3-D seismic data indicated that the deformation front reached at least 69º30'W (Boll et al., 2014).

Balgord and Carrapa (2016), through a sedimentological analysis involving U-Pb detrital zircon provenance in depocenters located at 35ºS, recorded a 25-30 Myr unconformity between the Bajada del Agrio and Neuquén Groups (Fig. 2). This was interpreted as related to the transition from a post-rift thermal subsidence to forebulge erosion during initial flexural loading linked to crustal shortening at 97 ± 2 Ma. Folguera et al. (2015) supported field observations through apatite fission track analysis in representative structures of the Malargüe fold-thrust belt, documenting an exhumation episode in Late Cretaceous times (Fig. 3a, 3d and 3e). Nevertheless, fission tracks data analyzed by these authors present significant dispersion. Finally, this proposed timing of shortening matches the rapid flexural accommodation revealed by sediment accumulation histories in the Cretaceous foreland basin (Horton et al., 2017; 2018).

2.2. Late Cretaceous deformation in the Agrio and Chos Malal fold-thrust belts

The Agrio and Chos Malal fold-thrust belts are located further east in the Argentinian side of the Andes and south of the Malargüe fold-thrust belt (Figs. 1 and 4). These belts are characterized by mixed styles of deformation with a western thick-skinned area product of tectonic inversion of the Mesozoic Neuquén Basin and an eastern part dominated by thin-skinned structures (see Rojas Vera et al., 2015 and references therein). Studies developed in the non-

marine deposits of the Neuquén Group in these fold-thrust belts demonstrated the synorogenic character of this unit supporting the interpretation of a foreland basin stage in the Neuquén Basin since the Late Cretaceous (Ramos, 1981a; Zamora Valcarce et al., 2007, 2009; Tunik et al., 2010; Di Giulio et al., 2012, 2016). Particularly, throughout the entire Agrio fold-thrust belt (Fig. 1), an unconformity between the Neuquén and the Bajada del Agrio groups has been widely documented, being more significant in the western part of the belt, and loosing expression towards the frontal structures (Groeber, 1946; Ramos and Folguera, 2005; Leanza, 2009) (Fig. 2). Changes in thickness in the Neuquén Group were detected in subsurface by Cobbold and Rosello (2003), indicating Late Cretaceous activity along a thrust located in the frontal sector, defining it as a Late Cretaceous fold-thrust belt mildly reactivated in Miocene times (Ramos and Folguera, 2005). Additionally, Zamora Valcarce et al. (2006) dated a series of igneous rocks intruding folded structures in the area, constraining a Late Cretaceous deformation between ~100 and ~73 Myr. Later, Zamora Valcarce et al. (2007) confirmed, based on paleomagnetic studies, that one of these igneous rocks intruded a previously deformed sequence, which was shortened during Miocene times. Late Cretaceous contraction in the Agrio and Chos Malal fold-thrust belts has been recently supported through thermochronological studies by Rojas Vera et al. (2015). These authors published the results of a fission tracks analysis performed in the inner structures of these belts, which indicated a regional exhumation episode at ~70 Ma, younger than the one registered in the frontal structures of the Agrio fold-thrust belt at ca. ~100-95 Myr (Zamora Valcarce et al., 2009). These data indicated a 6 km exhumation at ~69 Ma (Ramos and Folguera, 2005), calculated from the cooling age of a Permian pluton (Kay et al., 2006). However, fission tracks data presented by Rojas Vera et al. (2015) show a large dispersion and additional thermochronological data is still needed in order to corroborate their interpretations.

More recently, Horton and Fuentes (2015) suggested that the ~60-40 Myr interval was a time of neutral tectonic regime based on the observation of slowing sediment accommodation in the Neuquén foreland basin stage. However, determinations of La/Yb ratios in 70 to 42 Myr arc rocks by Spagnuolo et al. (2012) indicated increasing crustal thickening at those times. In this line, structural evidences for Eocene contraction from 36º to 37º30'S have been reported in several studies (Cobbold and Rosello 2003; Charrier et al., 2007; Sagripanti et al., 2012; Álvarez Cerimedo et al., 2013; among others).

Finally, Di Giulio et al. (2016) interpreted, through multi-proxy provenance data and lag times derived from apatite fission track analysis, a rapidly exhuming source within the Andes to the west in response to the Late Cretaceous deformational phase.

2.3 Late Cretaceous deformation in the Aluminé fold-thrust belt

The Aluminé fold-thrust belt extends to the south between 38º and 40º30'S from the North Patagonian Andes in the west to a distal deformed foreland sector known as the Neuquén Pre-cordillera in the east (Fig. 4).

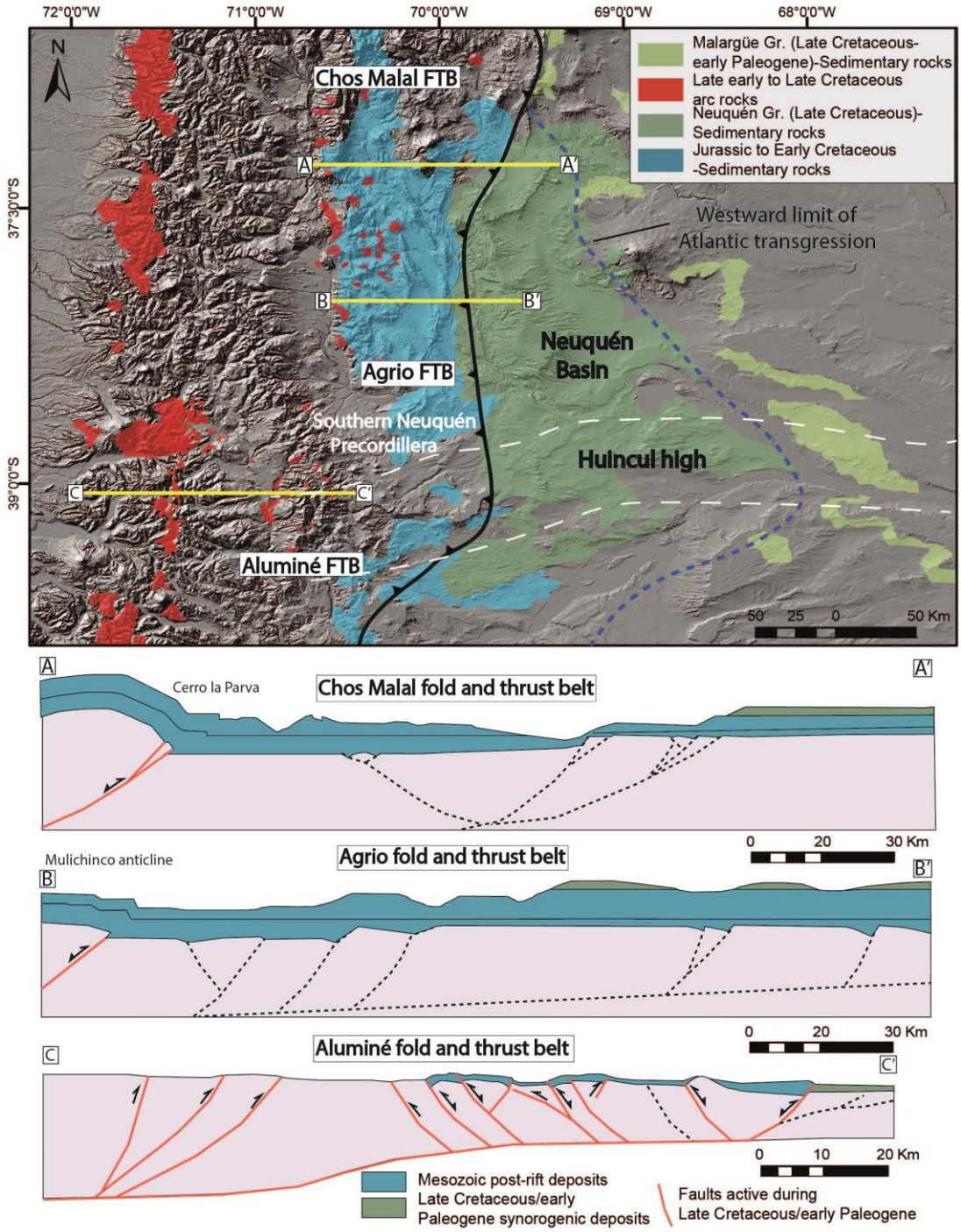

Fig. 4. DEM showing the location of the Chos Malal, Agrio and Aluminé fold-thrust belts. Cross-sections reconstructed to the Late Cretaceous/Paleogene contractional stage are taken from García Morabito and Ramos, (2012) and Rojas Vera et al. (2015).

In comparison to previous analyzed thrust belts, the Aluminé fold-thrust belt has been significantly less studied. Nevertheless, most recent studies shed some light into its earliest evolutionary stages. This thick-skinned belt was also affected by Late Cretaceous contraction that deformed early Mesozoic rift and post-rift deposits of the southwestern Neuquén basin, triggering synorogenic deposition of the Neuquén and Malargüe Groups (Fig. 2) in a foreland basin (Garcia Morabito and Ramos, 2012). Notably, during the Late Cretaceous phase, deformation propagated distally to the foreland uplifting an intraplate belt known as the Southern Neuquén Precordillera whose relief prevented the Atlantic transgression in Maastrichtian-Danian times (Fig. 4). This eastern area developed separately from the main Andes through positive inversion of Mesozoic rift depocenters and basement involved faulting (Garcia Morabito and Ramos, 2012). These deformed Mesozoic successions were covered by magmatic rocks with arc-affinities dated between ~75 and ~71Myr, indicating that mountain-building processes coexisted in space and time with an eastward arc-migration, and that this belt was mostly built in Late Cretaceous times (Garcia Morabito and Ramos, 2012). Finally, a Miocene-Pliocene contractional phase induced the reactivation of the internal and external sectors of the fold-thrust belt with minor propagation toward the foreland.

2.4 Late Early Cretaceous contraction in the North Patagonian fold-thrust belt (~42-44° S)

The North Patagonian Andes between 42°-44°S correspond to an orogenic segment characterized by a low topography Cordillera (<2000 m) in the west and the "Patagonian broken foreland" to the east (Bilmes et al., 2013) (Fig. 5). In this segment of the Southern Central Andes, the construction of the fold-thrust belt (Ramos and Cortés, 1984) has been originally related to a Neogene stage of deformation (e.g., Giacosa et al., 2005; Orts et al., 2012b).

The extra-Andean domain, with a wide geological record in the NNW-trending ranges forming the broken foreland, has also been interpreted as absorbing contraction since Neogene times after a protracted Mesozoic-Paleogene extensional regime (Fígari, 2005; Bilmes et al., 2013). However, recent studies have documented a late Early to Late Cretaceous contractional stage that uplifted the North Patagonian fold-thrust belt near the plate margin and the Patagonian intraplate sector to the east (Orts et al., 2012b; Echaurren et al., 2016a; Savignano et al., 2016).

The cordilleran sector is composed mainly by Mesozoic magmatic units, namely the North Patagonian Batholith and its cogenetic volcanic arc associations known as the late Early Cretaceous Divisadero Group (Fig. 2). The batholith has been primarily formed by I-type, calcal-

kaline granitoids of Jurassic-Cretaceous age with Neogene suites of less differentiated units (Pankhurst et al., 1992, 1999). The Mesozoic volcanic units consist of volcanic-volcanoclastic packages of rhyolithic ignimbrites, acid domes and andesite-basalt lava flows (Lago La Plata Formation) and mainly rhyolithic lithic tuffs (Divisadero Group). Between these units, isolated sedimentary rocks of the shallow marine to delta sequences of the Neocomian Coyhaique Group (part of the Río Mayo Embayment, or Aysén Basin; Aguirre-Urreta and Ramos, 1981; Suárez et al., 1996) are scattered and uplifted in the Andean eastern slope (e.g., Suárez et al., 2009a; Orts et al., 2012b). Even though these deposits are better exposed to the south, at ~45-46° S, their presence in the proto-Andean margin and toward the foreland account for periods of backarc basin formation in Jurassic to Early Cretaceous times (Orts et al., 2012b; Echaurren et al., 2016a,b).

In the cordilleran zone, the Situación Range exposes thick successions of the Lago La Plata Formation, covered by discontinuous outcrops of the Divisadero Group (Fig. 5b). Echaurren et al. (2016a) identified wedges with synextensional geometries controlling deposition of the Lago la Plata Formation volcanic layers, as fault-bounded horizons increasing dipping angles toward the base (Fig. 5b). Jurassic strata are unconformably underlying the Divisadero Group, as evidenced by a tight fault-propagated syncline (Fig. 5b). In the Pirámides and Galeses ranges, to the west and south respectively, deformed beds of the Neocomian Coyhaique Group are unconformably covered by the Divisadero Group, constraining this event to the early Aptian (Echaurren et al., 2016b). The presence of this regional angular unconformity has been interpreted as caused by initial contraction of the North Patagonian fold-thrust belt (Orts et al., 2012b; Echaurren et al., 2016a,b). After this contractional event, in Late Cretaceous times (~100–80 Myr), fission-track ages indicate that the forearc region exhumed from depths of at least 10–12 km (Duhart and Adriasola, 2008). The broken foreland domain is characterized by a series of ~N-trending belts exposing mainly Paleozoic and Mesozoic sedimentary and volcanic rocks, whose exposure is masked by two principal geological features; the Paleocene-Eocene bimodal volcanic rocks of the Pilcaniyeu Belt (Rapela et al., 1983; Aragón et al., 2011) and the Mesozoic Cañadón Asfalto Basin (Fig. 2).

The Cañadón Asfalto Basin contains thick nonmarine deposits of Jurassic sedimentary-volcanic rocks deposited in an extensional system controlled by a complex arrangement of depocenters (Fígari, 2005). The Cretaceous infilling corresponds to the Chubut Group (late Early to Late Cretaceous), which has been separated in the area into two units, the basal Los Adobes Formation (Aptian) and the Cerro Barcino Formation (Albian) to the top, composed by nonmarine and fluvial-lacustrine facies with variable volcaniclastic inputs (Fig. 2).

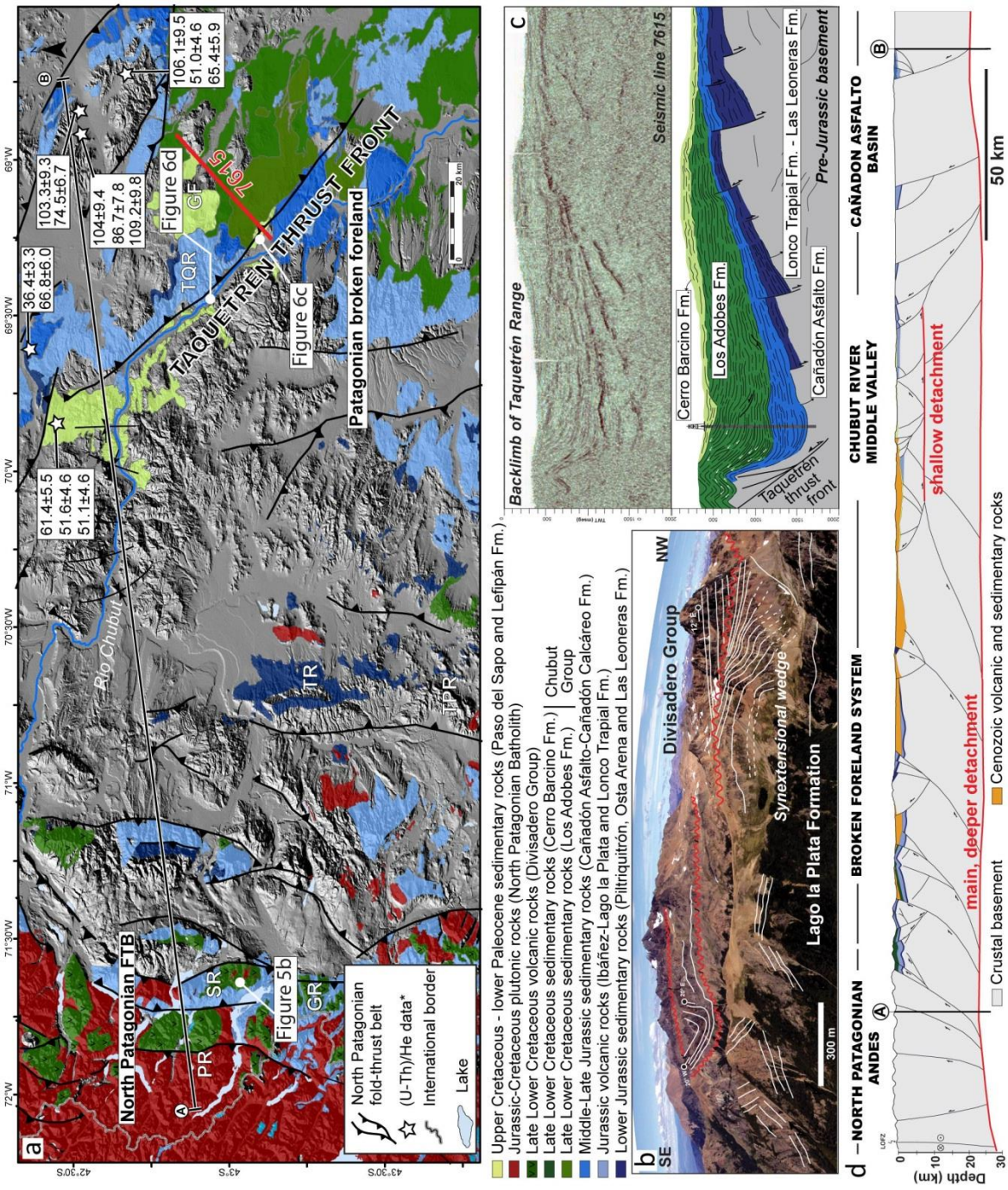

Fig. 5. a) DEM of the Patagonian Andes and the broken foreland sector showing the location of synorogenic deposits of the late Early Cretaceous Chubut Group, the Upper Cretaceous Paso del Sapo and the Danian Lefipan formations and Cretaceous arc-related volcanic and plutonic rocks (Echaurren et al., 2016a). Thermochronological (U-Th)/He data of the foreland region taken from Savignano et al. (2016). Abbreviations are: PR: Pirámides Range, SR: Situación Range, GR: Galeses Range, TR: Tecka Range, TPR: Tepuel Range, TQR: Tauqetrén Range, GF: Gorro Frigio area. b) Partially inverted wedge-like depocenters of Mid to Late Jurassic sections of the Lago La Plata Formation and late Early Cretaceous

contractional structures in the Situación Range, unconformably covered by Early Cretaceous volcanic rocks (Divisadero Group) (42°59'24.07''S/71°39'03.7''W) (Echaurren et al., 2016a).c) Subsurface growth-strata evidences in the Chubut Group (seismic line 7615 in a). d) Balanced structural cross profile (Echaurren et al., 2016a).

These units have been traditionally interpreted as sag deposits, or part of a synextensional reactivation of the basin (e.g., Fígari, 2005). More recently, Echaurren et al. (2016a) documented the presence of subsurface and surface contractional growth-strata highlighting their origin under a contractional regime (Fig. 5c and 6a-b).

In Late Cretaceous-Early Paleocene times, an Atlantic transgression covered the eastern Patagonian platform forming an embayment in the Taquetrén range zone (Scasso et al., 2012). These sedimentary units are the fluvial to tide-influenced estuarine rocks of the Paso del Sapo Formation (Late Cretaceous) and the open marine deposits of the Lefipán Formation (Danian), which were both also interpreted as part of the sag sequence (Figari, 2005) (Fig. 2). Nevertheless, field relations exhibit syncontractional growth-strata in both units. In the Gorro Frigio range, the Paso del Sapo Formation presents an overturned west-vergent fan of progressive unconformities in the footwall of a westward vengent thrust (Echaurren et al., 2016a) (Fig. 6c). U/Pb dating of a tuffaceous level in the growth strata constrained the depositional age to ~83 Ma, with detrital material provided by the Chubut Group with an age peak of ~117 Ma (Fig. 6c). The Chubut Group age population in the Paso del Sapo Formation probably suggests basin cannibalization during deposition of this unit (Echaurren et al., 2016a). Similar structural relationships are present to the north in Taquetrén range, where the shallow marine Lefipán Formation lies beneath Early Jurassic deposits by a reverse fault contact with the former unit presenting westward vergent progressive unconformities (Fig. 6d). These evidences account for a Late Cretaceous-Paleocene contractional reactivation of the western edge of the Cañadón Asfalto basin that correlates with the reactivation of the cordilleran area to the east. Recent, apatite (U-Th)/He ages in the broken foreland sector between 41°30'-43°S, support previous tectonic interpretations evidencing a Cretaceous to Paleogene exhumation event (~110-50 Myr) (Savignano et al., 2016) (Fig. 5a).

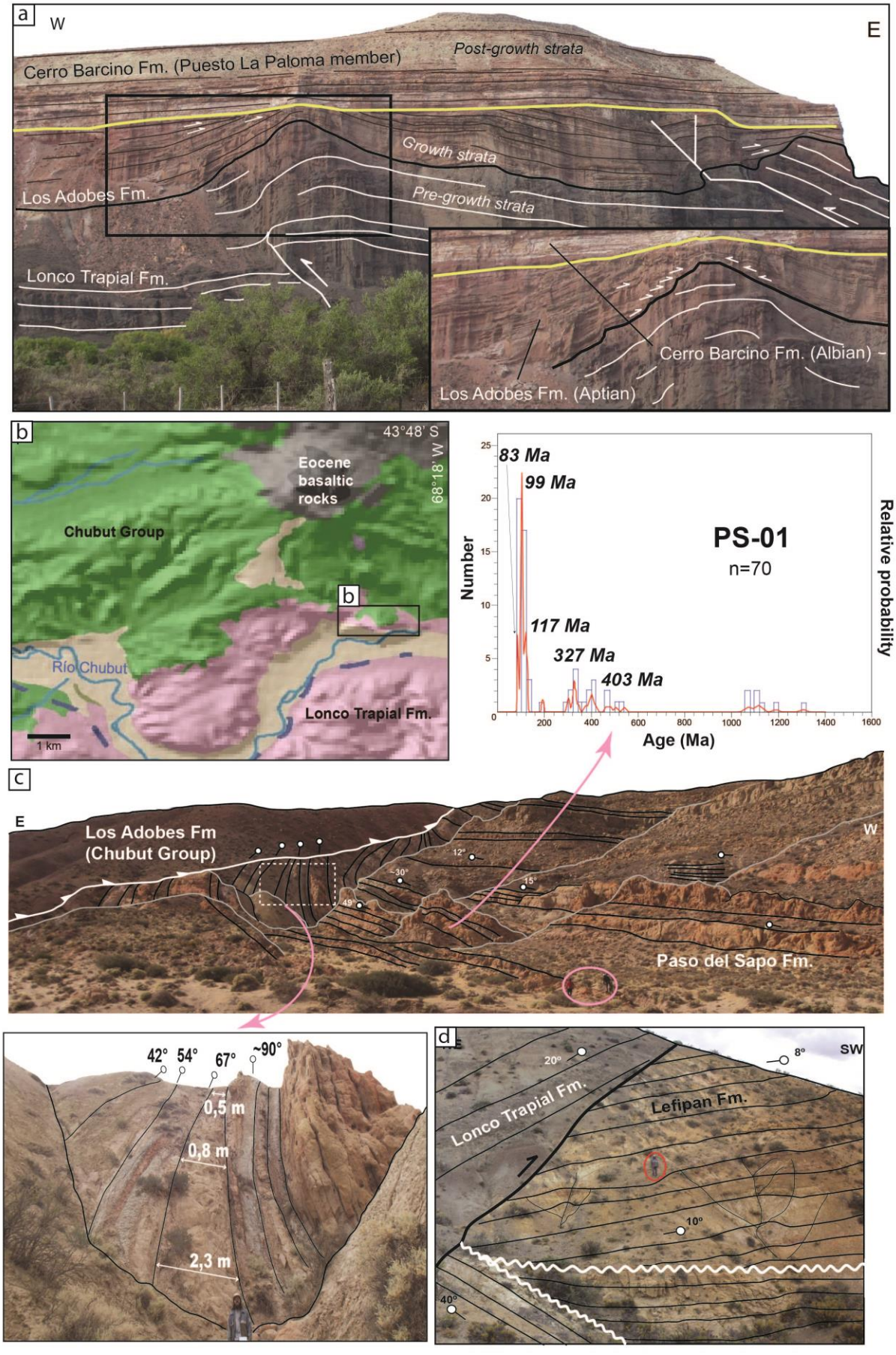

Fig. 6. a) and b) Aptian-Albian angular unconformity and syn-contractional growth-strata in the Aptian Los Adobes Formation at Los Altares location (43°51'15.35''S/68°20'26.36''W). c) Example of contractional growth-strata in the Paso del Sapo Formation dated through U/Pb in ~83 Ma at the Taquetrén thrust-front (43°04'56.18''S/69°|3'28''W). d) Example of contractional growth-strata in the shallow marine Lefipán Formation (42°57'10''S/69°25'06''W). See locations in Fig. 5a. Fig. modified from Echaurren et al. (2016a)

2.5 Late Early Cretaceous uplift of the North Patagonian Andes between 44º-46ºS.

The North Patagonian Andes between ~44-46°S differ morphologically from the latter northern segment. At these latitudes, the cordilleran domain is clearly separated from the broken foreland area through a 250 km broad, practically undeformed, continental sector (Fig. 7). In this segment of Central Patagonia, Jurassic to Cretaceous Western Gondwana breakup processes led to the development of the nonmarine San Jorge Gulf Basin in the intraplate sector and the marine to nonmarine Río Mayo Sub-Basin or Aysén Basin in an intra-arc and to retro-arc position (Uliana et al., 1989; Aguirre-Urreta and Ramos, 1981; Suárez et al., 2009a) (Figs. 2 and 7). The Río Mayo Sub-basin and San Jorge Gulf Basin were progressively inverted during Andean orogeny and constitute part of the Andes and broken foreland sectors respectively (Fig. 7). Particularly, the Río Mayo Sub-basin underwent a major reorganization during Aptian times reflected by the retreat of the Panthalasan sea to the west and the appearance of subaereal subduction-related magmatism of the Divisadero Group and equivalents units, identified from 42° to 49°S (Suárez et al., 1996, 2007, 2009a and references therein; Suárez et al., 1996; Parada et al., 2001). U–Pb SHRIMP zircon ages in this unit range between ~118 to 102 Myr (Pankhurst et al., 2003; Suárez et al., 2009b). The angular unconformity at the base of this unit is thought to reflect the earliest uplift episode of the North Patagonian Andes (Ramos, 1981b). This orogenic event is well recorded in the east-vergent Lagos La Plata and Fontana fold and thrut belts (Iannizzotto et al., 2004; Folguera and Iannizzotto, 2004). Unlike in the northern sector of the North Patagonian Andes (previous section), a preserved stratigraphic record constrained through U/Pb zircon ages, allowed restricting this episode to the 121-118 Myr time interval (Aptian) (Ramos, 1981b; Iannizzotto et al., 2004; Folguera and Iannizzotto, 2004; Suárez et al., 2009a). An additional Late Cretaceous tectonic pulse has been interpreted based on the description of a gentle angular unconformity between Latest Cretaceous calcalkaline volcanics and the Aptian Divisadero Group (Demant et al., 2007; Suárez et al., 2009a).

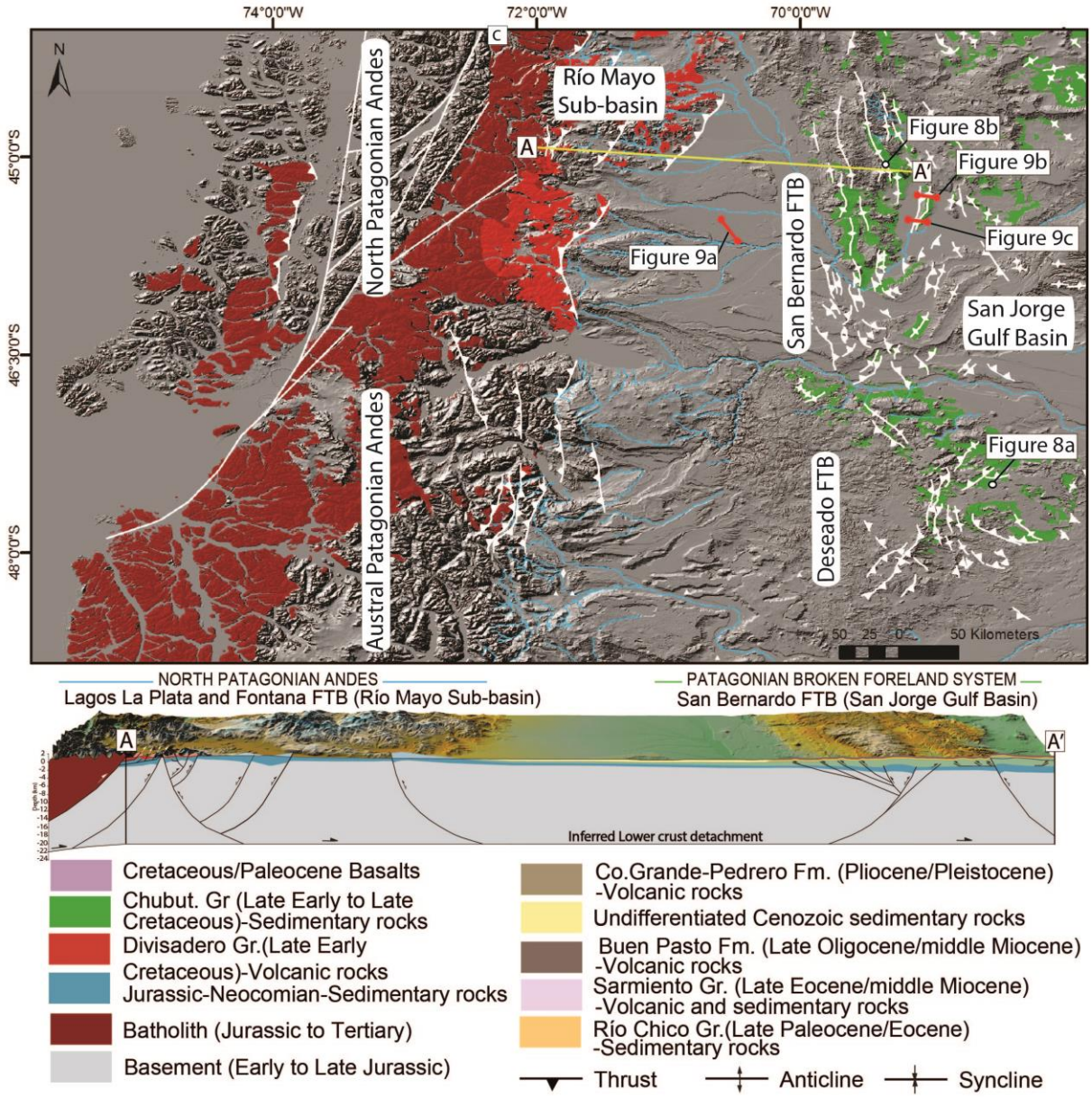

Fig. 7. DEM showing the southern sector of the North Patagonian Andes, the central and southern areas of the broken foreland sector (San Bernardo and Deseado fold belts). Below is a regional cross section from Gianni et al. (2017).

This event is supported by regional observations such as out-of-sequence thrusting in the Patagonian batholith in the Lago La Plata-Fontana fold-thrust belt and more locally by a K–Ar date of 105 Ma from cataclastic plutonic rocks (Iannizzotto et al., 2004; Folguera and Iannizzotto, 2004; Suárez and De la Cruz, 2001; Suárez et al., 2009a). Moreover, this tectonic pulse is coincident with the climax of tectonic emplacement of the Patagonian batholith at 98±4 Ma proposed by Ramos (1982). In concordance with above mentioned structural observations, Tunik et al. (2004) interpreted an exposure of the volcanic arc roots over the cordillera in late

Early Cretaceous times, based on a study of detrital modes in discrimination diagrams analyzing Cretaceous foreland deposits of the Chubut Group. East of the southern domain of the North Patagonian Andes, the Central sector of the Patagonian broken foreland uplifted as a product of tectonic inversion of Jurassic to Neocomian extensional depocenters (Homovc et al., 1995; Peroni et al., 1995). This intraplate belt is here characterized by the NNW-SSE-trending San Bernardo fold-thrust belt that exposes the western border of the San Jorge Gulf Basin and the Deseado fold belt to the south that deformed previous Permian to Jurassic extensional depocenters (Giacosa et al., 2010) (Fig. 7). As in the northern segment of the Patagonian broken foreland, the San Bernardo fold-thrust belt also presents extensive outcrops of the late Early Cretaceous to Late Cretaceous nonmarine Chubut Group (Fig. 2). Here, these rocks are characterized by a high proportion of distal, ash-fall deposits reworked in lacustrine and fluvial settings (Tunik et al., 2004). This succession is stratigraphically arranged as follows: The Pozo D-129 / Matasiete, Castillo, Bajo Barreal, Laguna Palacios and Colhué Huapi Formations, ranging in age from Aptian to late Cenomanian-Maastrichtian (?) (121.5-98 Myr) based on fossil records and U/Pb zircon data (Fitzgerald et al., 1990; Suárez et al., 2014; Allard et al., 2015) (Fig. 2). In the Deseado fold belt, César et al. (2011) and Pérez Loinaze et al. (2013) constrained the age of a partially equivalent unit to the base of the Chubut Group, known as the Baqueró Group, through U/Pb detrital zircons to the ~118-114 Myr time interval (Fig. 2). Surface and subsurface description of a regional angular unconformity along the Patagonian foreland region at the base of the Chubut Group has been commonly related to intraplate contraction and/or traspression (Clavijo, 1986; Barcat et al., 1989; Homovc and Constantini, 2001; Giacosa et al., 2010; Ranalli et al., 2011, among others) and has been directly linked with the initial growth of the North Patagonian Andes (Barcat et al., 1989; Ramos, 1981b; Iannizzotto et al., 2004; Folguera and Iannizzotto, 2004; Suárez et al., 2009a) (Fig. 8a). More recently, in the northern part of the Southern Patagonian Andes, Ghiglione et al. (2013) have dated by U/Pb detrital zircons in synorogenic deposits of Río Belgrano and Río Tarde formations, obtaining a similar maximum depositional age of ~122 Ma and ~118-111 Myr respectively. These detrital zircon population yielded interesting results. Instead of presenting a clear Andean provenance, they mostly come from the Patagonian foreland. Hence, the authors pointed out that their data could indicate a late Early Cretaceous post ~122 Ma uplift of the Deseado fold belt and the western edge of the North Patagonian Massif. Particularly, uplift of the San Bernardo fold-thrust belt is further supported by seismic surveys and surface detection of growth-strata that described a synorogenic character of the Chubut Group

(Barcat et al., 1989; Navarrette et al., 2015; Allard et al., 2015; Gianni et al., 2015a,b) (Figs. 8 and 9).

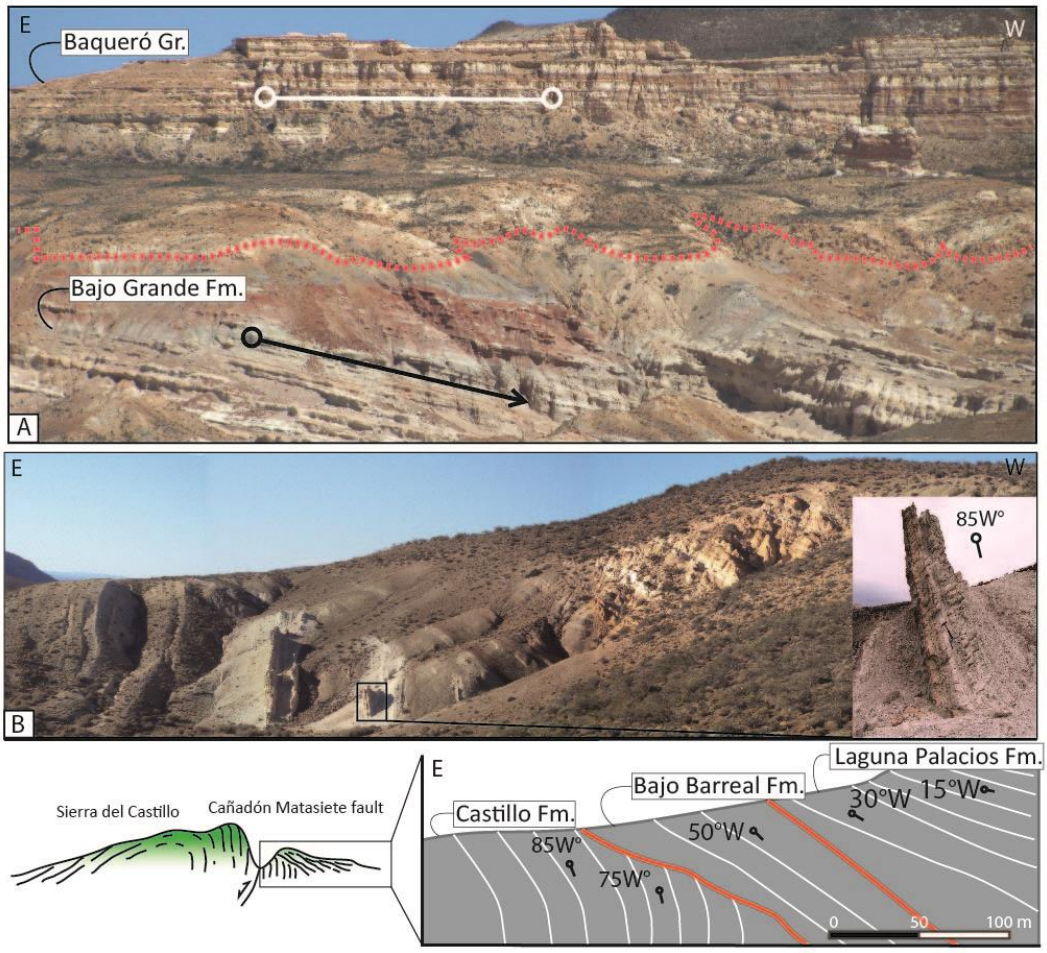

Fig. 8. a) Image of the Bajo Grande unconformity evidencing an Aptian tectonic event in the Deseado fold belt (47°51'S/68°46'W) (modified from Giacosa et al. 2010). b) Example of surface evidences of growth strata in late Early to Late Cretaceous units of the Chubut Group in the San Bernardo fold-thrust belt (Patagonian broken foreland) (45°07'57.43"S/64°18'18"W). See location in Fig. 7 ((modified from Gianni et al. (2015a)).

In the Deseado fold belt a paleo-stress analysis carried out by Reimer et al. (1996) concluded that this area has been under compression since late Early Cretaceous. Later identification of an Aptian angular unconformity of regional character by Giacosa et al. (2010) confirmed the beginning of contraction in this fold-thrust belt (Fig. 8a). Across the foreland and offshore areas, the Chubut Group is capped by a regional angular unconformity, either by retroarc basalts or clastic deposits of Upper Cretaceous/Paleogene age, attesting for a major intraplate contractional event in latest Cretaceous times (Feruglio, 1949; Lesta et al.,1980; Constinanzia et al., 2011; Micucci et al., 2011; Navarrette et al., 2015).

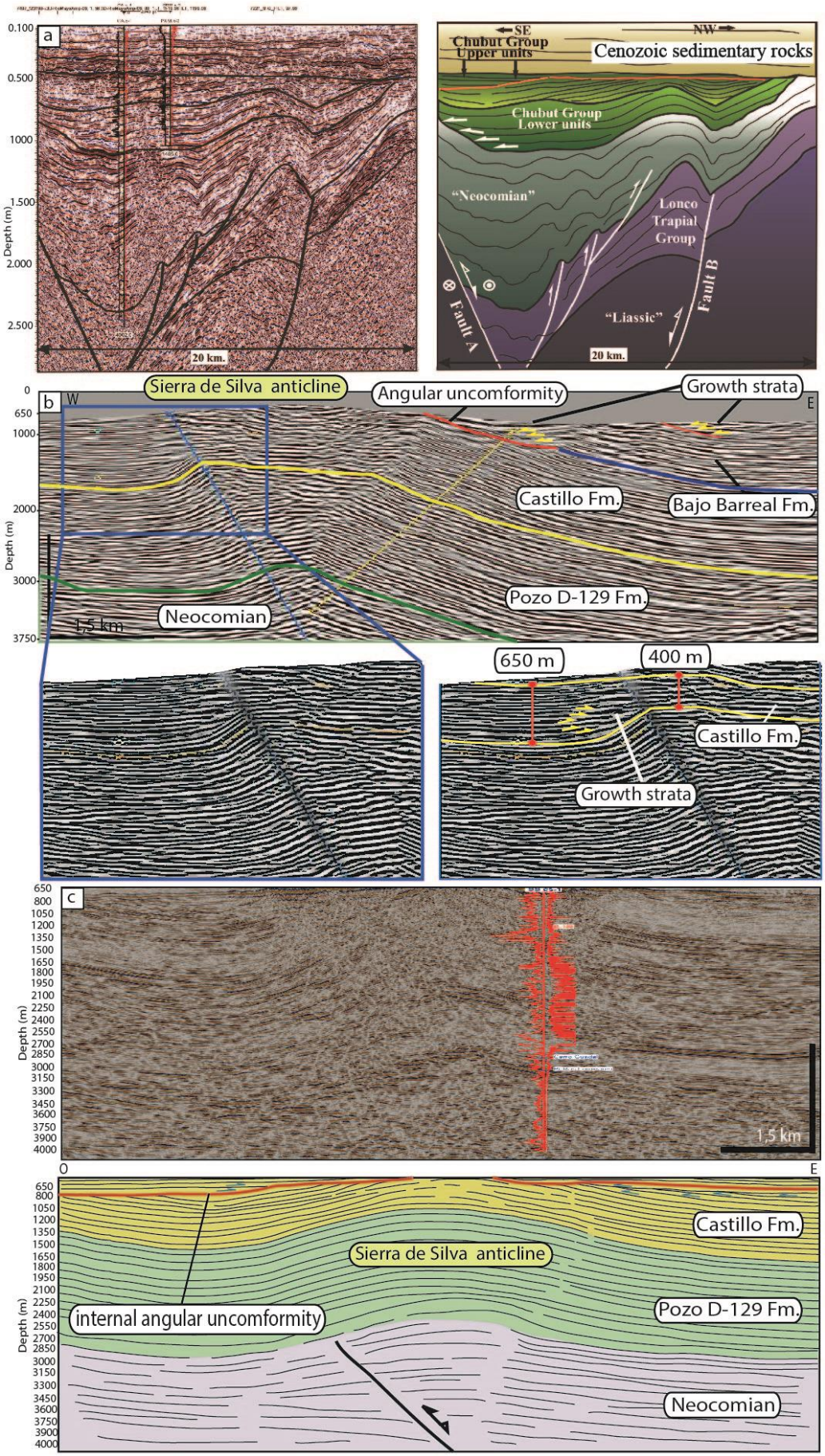

Fig. 9. Seismic reflection lines showing examples of growth-strata in late Early to Late Cretaceous units of the Chubut Group in (a) Aptian to Cenomaninan syncontractional units in the eastern sector of the Rio Mayo sub-basin from Navarrete et al. (2015) and (b) Albian to Cenomanian syncontractional in the Sierra de Silva anticline in the easternmost San Bernardo fold belt. See locations in Fig. 7.

---

3. Magmatic arc behavior during Cretaceous Andean construction

Abnormal eastward arc expansions in individual segments along the Southern Central Andes from 36°S to 48°S have been broadly documented during early Andean orogenic stages from Cretaceous to Paleogene times (Barcat et al., 1989; Ramos and Folguera, 2005; Kay et al., 2006; Suárez et al., 2009a; Folguera and Ramos, 2011; Spagnuolo et al., 2012; García-Morabito and Ramos, 2012; Fennell et al., 2015; Gianni et al., 2015a; Echaurren et al., 2016a; Folguera et al., 2015). In this section, the regional spatial and temporal evolution of arc magmatism is analyzed following the approach of Coney and Reynolds (1987), where arc rocks ages are plotted against the distance perpendicular to the trench. To do so, we used previous and new datasets of available radiometric ages (U/Pb, Ar/Ar, K/Ar, Rb/Sr) from Cretaceous plutonic and volcanic arc-related rocks between 36º-49ºS (see caption on Fig. 10 and 11 for detailed references of datasets).

The magmatic arc between 36°S to 40°30'S underwent eastward migration in late Cretaceous to early Eocene period, during the initial development of the Malargüe, Chos Malal, Agrio and Aluminé fold-thrust belts (Llambías and Rapela, 1989; Franchini et al., 2003; Kay et al., 2006; Ramos and Folguera, 2005; Zamora Valcarce et al., 2006; García Morabito and Ramos, 2012; Spagnuolo et al., 2012; Folguera et al., 2015, Rojas Vera et al., 2015, Fennell et al., 2015; Di Gulio et al., 2016; Horton and Fuentes, 2016) (Fig. 10a). As reviewed in the work of Fennell et al. (2015), initial arc migration at 36° to 38°S latitudes is marked by a Late Cretaceous to Eocene arc offset on the Chilean side of the Andes respect to the Late Cretaceous arc north of 35°30'S (see Fig. 3.32; Charrier et al., (2007)) (Fig. 10a and b). In this regard, Tunik et al. (2010), based on the analysis of the Mesozoic detrital zircons from the Neuquén Group, showed that there are two important peaks in the volcanic arc activity developed at 110 and 125 Ma respectively, followed by a gradual decrease, interpreted as a an arc waning stage. Detrital zircon data shown by Di Giulio et al. (2012), Fennell et al. (2015), Balgord and Carrapa (2016) and Horton and Fuentes (2016) agree with this waning in arc activity between ~100 and ~85 Myr. Volcanic arc rocks to the east in the Argentinian Andean slope, have ages between ~85 and ~60 Myr (Domínguez et al., 1984; Munizaga et al., 1988; Llambías and

Rapela, 1989; Linares and González, 1990; Jordan et al., 2001; Franchini et al., 2003; Zamora Valcarce et al., 2006; Spagnuolo et al., 2012), with a few Eocene ages (Llambías and Rapela, 1989; Cobbold and Rossello, 2003) (Fig. 10a). This fact has been used to propose an eastward shifting of the arc front in Late Cretaceous to Paleogene times (Ramos and Folguera, 2005; Spagnuolo et al., 2012, Folguera et al., 2015) (Fig. 10a). Main aspects of this magmatic belt between 35°30' and 38°S have been summarized by Llambías and Rapela (1989), Franchini et al. (2003), Kay et al. (2006), Zamora Valcarce et al. (2006) and more recently by Spagnuolo et al., (2012). Chemical analyses show arc-like features indicated by high field strength elements (HFSE) depletion (La/Ta >28; Ta/Hf < 0,15) and fluid mobile element enrichment (Ba/La >20) (Kay et al., 2006; Zamora Valcarce et al., 2006). A southward continuation of this magmatic belt has been proposed by García-Morabito and Ramos (2012), based on an analysis of the igneous outcrops and a revision of previous and new radiometric data between 38°30'S to 40°30'S (Fig. 10a). At these latitudes, the authors identified a series of porphyric intrusive bodies of andesitic-rhyodacitic composition and associated extrusive series that were emplaced in close relation to NNW and NE-trending contractional structures. This spatial relation was interpreted as a syntectonic emplacement of igneous bodies or postectonic immediately after the Late Cretaceous contractional pulse (García-Morabito and Ramos, 2012). Geochemical data from outcrops of the Aluminé valley show typical volcanic arc signatures, indicated by trace elements ratios (La/Ta (33), Ba/La (20.35)), Nb negative anomalies, and a K, Rb, and Th enrichment with respect to N-MORB (Lagorio et al., 1998) that together reflect a ~170 to 200 km arc expansion in Late Cretaceous times (García-Morabito and Ramos, 2012) (Fig. 10a).

As seen in the presented time–space diagram in Fig. 10b, the eastward arc broadening between 36º to 40º30'S began between at 100-90 Myr showing a fast propagation at ~75 Ma. This migration would have reached a maximum distal position about 430-400 km from the trench at ~67-64 Myr, coevally with deposition of the uppermost levels of the Neuquén and Malargüe Groups (Llambias and Aragón, 2011, Aguirre-Urreta et al., 2011) (Fig. 10b). In this context, the Neuquén and Malargüe Groups would be the synorogenic sedimentary unit associated with an early Andean orogen developed during changing arc dynamics from ~100-90 to ~65 Myr (Ramos and Folguera, 2005; García Morabito and Ramos, 2012; Fennell et al., 2015; Horton and Fuentes, 2016) (Fig. 10b).

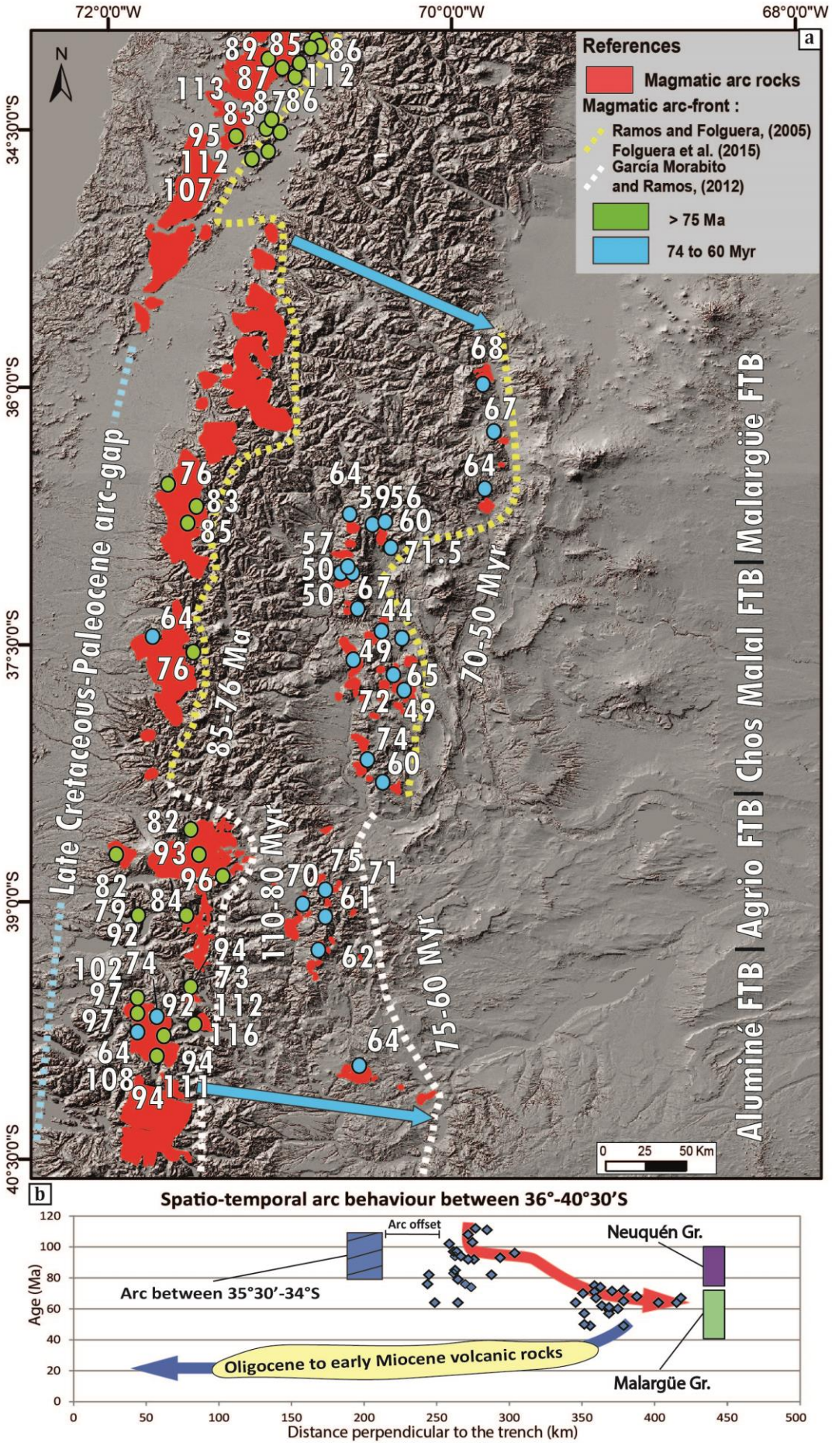

Fig. 10. a) Middle Cretaceous to Early Paleogene arc between 35° and 40°30'S. The reader is referred to Folguera et al. (2015) and García Morabito and Ramos, (2012) for complete references of the presented geochronological dataset. These datasets were complemented with ages from Suárez et al. (1986); Lara and Moreno (2004), Moreno and Lara (2008) and IIG/MMAJ/JICA (1978). b) Spatio-temporal analysis of arc magmatism showing an arc migration stage since around 100-90 Myr and its relation to synorogenic deposition.

Through a geochemical study in volcanic rocks at 35°30'S and a comparison with equivalents rocks between 35°-41°S, Iannelli et al. (2018) concluded that the expanded Late Cretaceous-Paleocene arc had a weaker arc-like signature and less slab-fluid influence in its northernmost extreme. This contrasting behavior along with the documentation of localized extensionally-controlled magma ascent in the hinterland of the Cretaceous orogen (Tapia, 2015; Fennell et al., 2017) has been explained by the development of an incipient slab window at 35º30′S around 70 Ma. In the entire 36°-40°30'S segment, arc retraction to the west took place from Oligocene to early Miocene times concomitant with the eruption extensive synextensional magmatism (Muñoz et al., 2000; Ramos and Folguera, 2005; Folguera and Ramos, 2011) (Fig. 11b).

Between 40°30'S to 44°30'S, eastward shifting of the magmatic front took place in late Early Cretaceous times to Latest Cretaceous followed by an early Paleocene magmatic shut-off (Folguera and Ramos, 2011; Echaurren et al., 2016a) (Fig. 11a).As shown in the time–space diagram in Fig. 11b, the eastward arc broadening began between 120-110 Myr reaching a distance up to 520 km from the trench at ~70 Ma.

Echaurren et al. (2016a) noticed that early contraction evidenced by an angular unconformity in the North Patagonian Andes was contemporaneous with the eastward expansion of the arc rocks of the Divisadero Group at ~118 Ma, as also observed in the southern sector of this belt by Gianni et al. (2015). Even though the magmatic suites of the North Patagonian Batholith are mainly concentrated in the North Patagonian Andes, satellite plutonic and volcanic units reached the foreland at ~90 Ma, evidencing an eastward expansion of the magmatic activity at 43°30'S from previous 136-124 Myr arc (Fig. 11a and b). These eastern bodies are calc-alkaline intermediate-to-acid volcanic rocks of the Don Juan Formation (K–Ar age of 91 ± 3 Ma; Franchi and Page, 1980) and I-type, calc-alkaline, basic-to-acid plutonic suites of the Lago Aleusco area (López de Luchi et al., 1992).

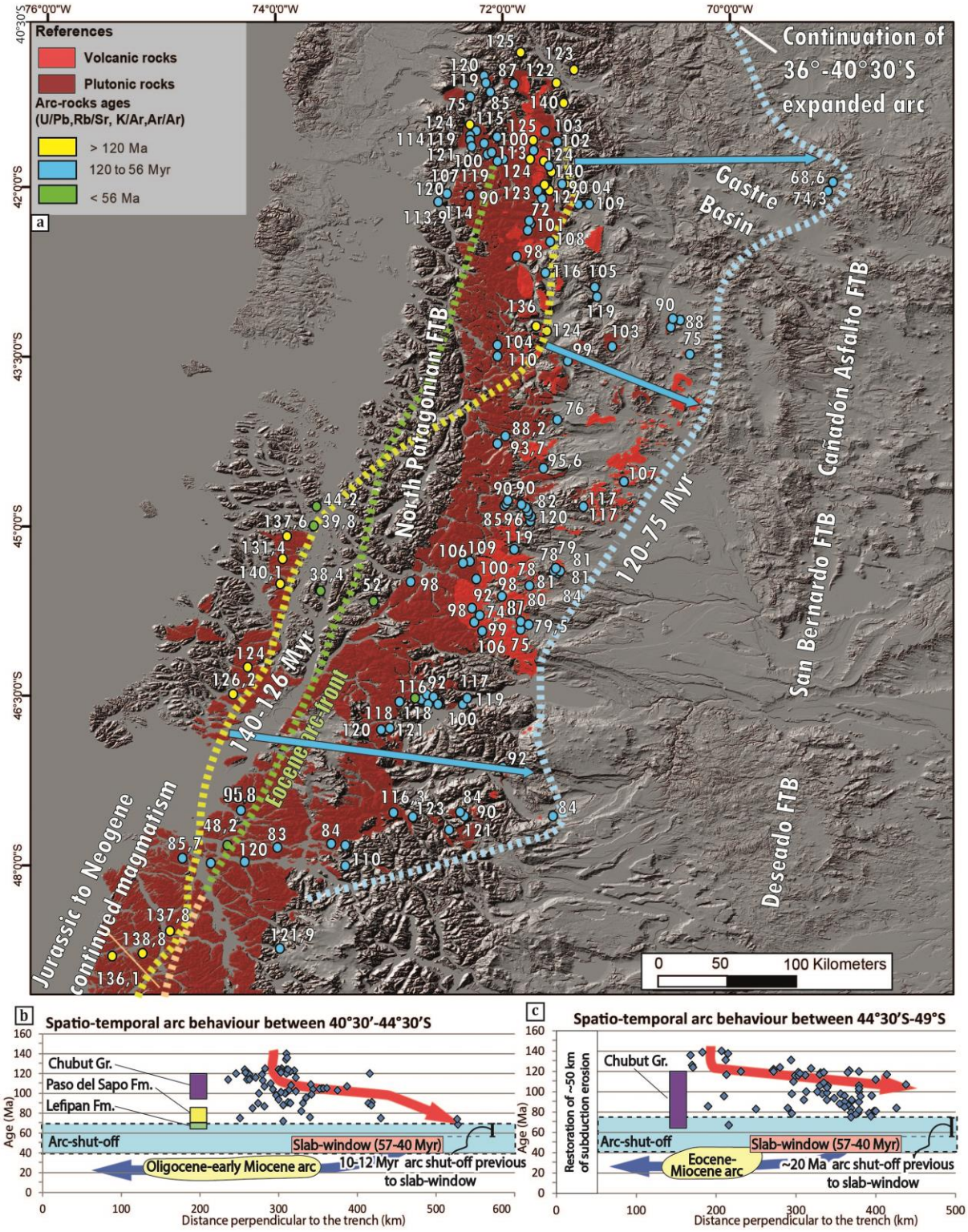

Fig. 11. a) Compiled radiometric dataset of arc rocks between 40°30'S to 49°S ranging in age from 140 to 40 Myr arc. References to ages from 40°30'S to 42°30'S are Adriasola et al. (2006), Aragón et al. (2011), Castro et al. (2011), Cazau et al. (1989), Ghiara et al. (1999), González Díaz (1979;1982), Haller and Lapido (1982), Halpern et al. (1975), Stipanicic and Toubes (1975), Linares and González (1990), Lizuaín (1979, 1980, 1981b, 1987), Pankhurst

et al. (1994), Pesce (1979), Rabassa (1978), Rapela et al (1983, 1987, 2005), SEGEMAR-JICA, Sepúlveda and Viera (1980), Soechting (2001), Toubes and Spikerman (1973), Vattuone and Latorre (2004), Varela et al. (2005) and Zaffarana et al. (2017). References to ages from 42°30' to 49°S can be found in Gianni et al. (2015a) and Echaurren et al. (2016a). This Fig. differs from the one presented by Gianni et al. (2015a) in which only the early Cretaceous arc, immediately before late Early to Late Cretaceous arc shifting, was plotted. b) and c) Spatio-temporal analysis of arc magmatism showing arc migration stages around 110 to 120 Ma and subsequent arc shut-off 10 to 20 Myr and its relation to synorogenic deposition. Trench position in c) was restored by ~50 km forearc erosion between 46° to 49°S in Neogene times (Guivel et al., 2003; Ramírez de Arellano et al., 2012).

According to Echaurren et al., (2016a), radiometric K–Ar ages of ~90–75 Myr of this plutonism (Turner, 1982) indicate a temporal association with retroarc deformation of the Taquetrén thrust front, where the ~83 Ma Paso del Sapo Formation deposited syntectonically (Fig. 11b). The easternmost expression of the eastward incursion of the magmatic activity is represented by arc-related calc-alkaline rocks emplaced in the Gastre Basin (Fig. 11a and b). Recently, these rocks have been dated in 68.6 Ma and 74.3 Ma by Zaffarana et al. (2017). The end of this period of magmatic expansion is marked by an arc waning since ~74 Ma evolving to an arc shut-off from 70 to ~57 Myr that developed coetaneous to the Maastrichtian–early Paleocene marine synorogenic deposits of the Lefipán Formation in flexural depocenters (Echaurren et al., 2016a) (Fig. 11b).

Gianni et al. (2015a), suggested that the latter arc migration continued southward from 44°30' to 48°S (Fig. 11 a). An abnormal arc expansion at these latitudes has been inferred since the pioneering work of Barcat et al. (1989) and its tectonothermal consequences have been analyzed in more recent studies (Suárez et al 2009a; Folguera and Ramos 2011; Gianni et al., 2015a). As seen in the time–space diagram of Fig. 11b, in this segment the eastward arc broadening began at ~120-122 Myr reaching a distance up to 440 km from the trench. This magmatic stage was followed by a period of magmatic waning since ~74 Ma (Gianni et al., 2015a) that ultimately evolved into a magmatic gap stage up to ~50 Ma (Suárez and de la Cruz, 2001) (Fig. 11b). Noteworthy, in this segment the paleo-trench position was reconstructed by taking into account ~50 km forearc loss in Neogene times (Guivel et al., 2003; Ramírez de Arellano et al., 2012) (Fig. 11b). The igneous rocks involved in this process have been grouped into several calc-alkaline units ranging from late Early Cretaceous silicic to mesosilicic rocks and Late Cretaceous basaltic to dacitic rocks that share typical arc signatures (Pankhurst et al., 1999; Parada et al., 2001; Demand et al., 2007). As initially suggested

in the pioneering work of Barcat et al. (1989), late Early Cetaceous arc expansion was concomitant with the synorogenic deposition of the Chubut Group in the foreland area (Fig. 11b). Most recent studies echoed this view and demonstrated that arc migration/expansion was coetaneous to the initial development of the Patagonian broken foreland (Gianni et al., 2015a; Navarrete et al., 2015).

In Paleogene times, the Aluk-Farallon mid-ocean ridge interacted with the Patagonian margin at analyzed latitudes producing a well-recognized slab window event. The latter, has been mostly inferred based on the presence of 57-40 Myr intraplate magmatism, scattered between 40°30' to 49°S, with geochemical signatures compatible with a primitive mantle sources and the development of a concomitant arc null (Ramos and Kay, 1992; Aragón et al., 2011).

Noteworthy, the documented arc waning-shut off stages described between 40°30' to 48°S preceded ridge collision by ~20 to 12 Myr, which hampers linking the volcanic null entirely to the formation of the slab window.

In the whole 40°30'-48°S segment, after the magmatic waning/gap period, the arc retracted to the west and reappeared in Late Eocene to early Miocene times during significant intraplate magmatic and extensional activity in the continental interior (Pankhurst et al., 1999, see Fig.6; Folguera and Ramos, 2011; Iannelli et al., 2017; Fernández Paz et al., 2017) (Fig. 11b).

4. Geodynamic controls behind arc expansions

Spatio-temporal changes in arc regions are controlled by a diversity of processes and identifying a dominant cause is often difficult. Any successful hypothesis for arc behavior between 36° to 47°30'S reviewed in this study, must explain key observations such as ~400-520 km magmatic migrations/expansions from the trench and arc quiescence stages lasting between 10 to 20 Myr in most of the analyzed segments (Fig. 10 and 11).

Significant across-arc migration patterns have been mostly attributed to changes in convergence rates, variations in slab dip, crustal thickening and absolute trench motion produced by subduction erosion or accretion, which are further influenced by structurally controlled magma ascent and emplacement (e.g., Von Huene and Scholl, 1991; Kay et al., 2005; Haschke et al., 2002; Mamani et al., 2010; Karlstrom et al., 2014).

Subduction erosion is expected to produce arc advance as the forearc area is reduced, while subduction accretion would generate arc retraction as the forearc region is enlarged. In both cases during arc shifting the magmatism remains relative active (Von Huene and Scholl, 1991; Kay et al., 2005). The fact that most arc-migrations/expansions reviewed in this work end with arc quiescence stages (10-20 Myr) described between 40°S to 47°30'S (Suárez and

De la Cruz, 2001; Gianni et al., 2015; Echaurren et al., 2016) impede subduction erosion as the main mechanism behind arc dynamics (Fig. 10b; Fig. 11). The chemistry of arc rocks has been used indirectly to infer subduction erosion as removed forearc crustal material enters the mantle wedge and contaminates the source of arc magmatism. Chemical signatures for this process involve a decrease in εNd values, increase in $^{87}Sr/^{86}Sr$ ratios, steeper REE patterns (higher La/Yb ratios); and higher Sr contents (Kay et al., 2005). Notably, such trace elements pattern and isotopic signatures are lacking in 120-80 Myr arc rocks (Weaver et al., 1990; Pankhurst et al., 1992, 1999; Kay et al., 2006; Hervé et al., 2007; Echaurren et al., 2016b) showing no evidence for significant source contamination and hence, Cretaceous subduction erosion at studied latitudes. Nevertheless, younger events of subduction erosion have been proposed from Oligocene to latest Miocene/Pliocene along the analyzed Andean segment (e.g., Kukowski and Oncken 2006; Guivel et al., 2003).

The convergence rate influences the advection of heat by corner flow in the mantle wedge and hence, it is expected to control arc-depth to slab, width and location. Molnar et al. (1979) suggested a direct relation between increased convergence velocities and wider volcanic arcs. However, most recent numerical modeling studies suggest that there is no clear correlation between convergence and the location of the melting region in arcs (Grove et al., 2009; 2010) or conversely to the early proposal of Molnar et al. (1979), there is a trenchward arc expansion with increasing rates (Karlstrom et al., 2014; Fig. 10a). Noteworthy, as high plate convergence took place along the entire active margin (Maloney et al., 2013) any possible effect related to high convergence rates in Cretaceous times must have been visible in the whole Andean margin and not just in the discrete segment between 36°S to 47°30'S described in this work (Fig. 12). Additionally, the convergence rate hypothesis faces a critical limitation to explain arc quiescence at the end of arc migration stages (Fig. 10b; Fig. 11).

Karlstrom et al. (2014) put forward a provocative model tested through a mathematical approach in which some arc migrations are dictated by changes in crustal thickness. According to this work, as crustal thickening proceeds, this drives arc migration as mantle wedge material is squeezed away from the trench. Particularly, in this model arc shut-off only takes place when crustal thickness surpasses the 70 km, a value comparable to the thickest orogens on earth (e.g., Tibetan and Puna-Altiplano plateaus). Although, we might expect some influence of this process in the study area, there is no geological or geochemical evidence (e.g., La/Yb ratios) for crustal thickening above 70 km during Cretaceous to early Cenozoic times necessary for driving the observed arc shut-off (e.g., Parada et al., 2001; Kay et al., 2006; Spagnuo-

lo et al., 2012; Echaurren et al., 2016b). Hence, arc migration/expansions terminating in arc quiescence in most of the analyzed area are not easily explained by crustal thickening alone.

Structurally controlled magma ascent could have contributed to some degree to the observed arc-migrations. However, field evidences attesting for such controls have not been provided so far. Additionally, the general thick-skinned structures in fold-belts between 36°S to 47°S, mostly related to high angle reverse faults, are not expected to substantially deflect the magmatic trajectory to explain the described arc-migrations/expansions. More importantly, this process also fails to explain the evolution from arc expansion to arc quiescence observed in most of the analyzed area in latest Cretaceous-Early Paleogene times.

Changes in slab dip linked to subducted plate shallowing is expected to expand the arc and shift its position towards the foreland area as the mantle wedge is pushed-forward and drive arc shut-off when full slab flattening is achieved (e.g., Coney and Reynolds, 1977; Dickinson and Snyder, 1978). This view is supported by recent numerical modeling and global analyses in subduction systems (Tatsumi and Eggins, 1995; Grove et al., 2009; 2012, Fig. 11a).

The slab shallowing hypothesis is potentially the most compatible with the arc behavior observed in Figs. 10 and 11 as it may explain the evolution from ~400-520 km arc migrations/expansions to final magmatic quiescence. Furthermore, slab flattening could be sustained for several millions of years independently of convergence rates, crustal thickening and forearc erosion or accretion. Most of tectonic studies in the reviewed area have argued in favor of changes in subduction angle linked to slab shallowing or flattening events as the most likely process to explain the observed arc behavior in the analyzed areas (Suárez et al., 2009a; Ramos and Folguera, 2005; Kay et al., 2006; Folguera and Ramos, 2011; García Morabito and Ramos, 2012; Spagnuolo et al., 2012; Gianni et al., 2015a; Echaurren et al., 2016). These studies have interpreted such episodes in terms of individual slab shallowing or flattening processes related to deformation in discrete retroarc fold-thrust belts. Nevertheless, as seen in Fig. 12a, the region that experienced arc migration/expansion forms a continuous belt from 36° to 48°S, which raises the possibility that a single large-scale slab flattening event could have taken place in Cretaceous to Paleogene times.

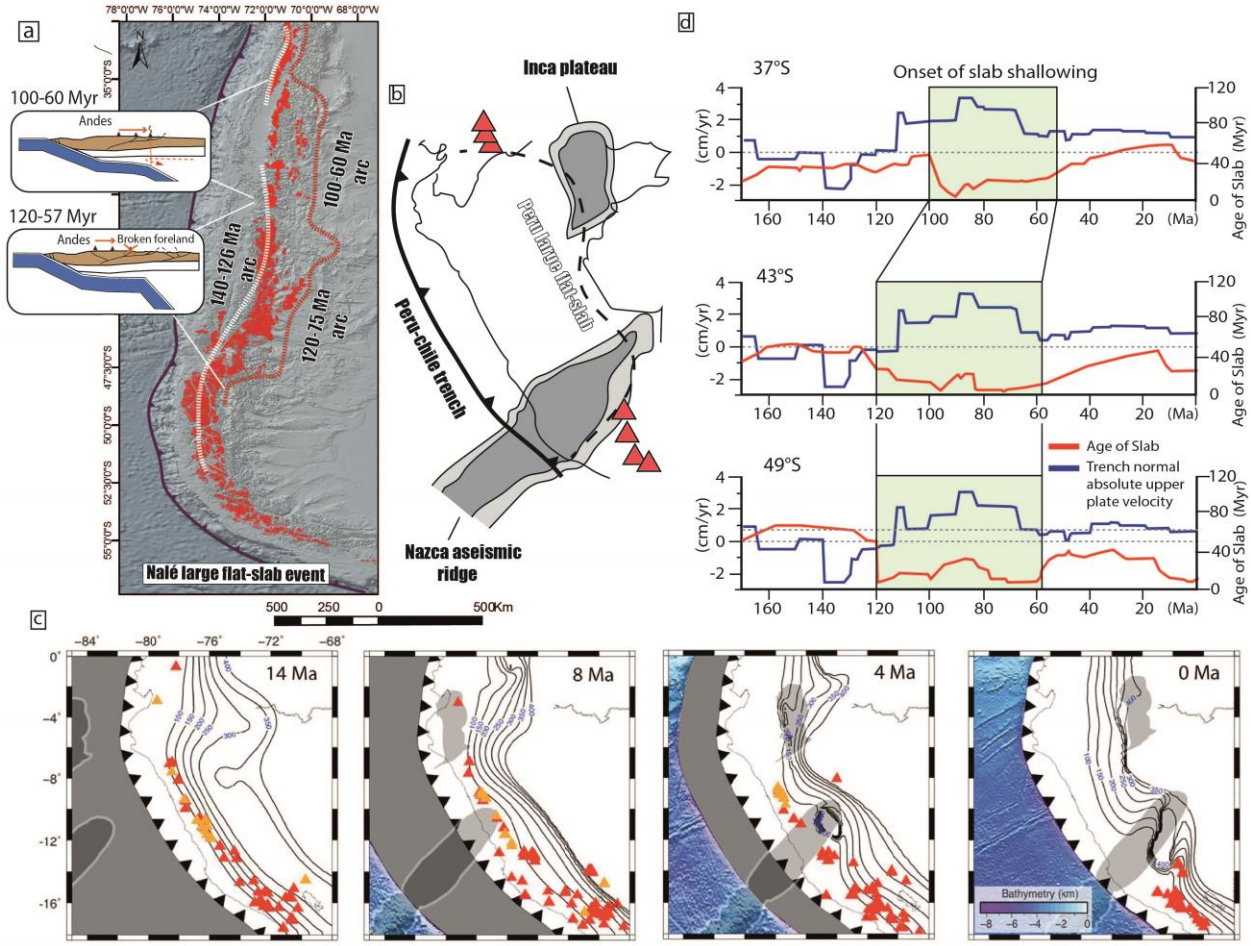

Fig. 12. a) Distribution of Cretaceous to Paleocene arc-related outcrops showing the potential extent of the Nalé large flat-slab. b) Image showing the Peruvian large flat-slab for comparison with the Nalé large flat-slab configuration proposed in this work. c) Compiled radiometric data set from Hu et al. (2013) showing arc positions during the development of the Peru large flat-slab. Please note the limited arc migration before magmatic shut-off during slab flattening in Peru. d) Diagram showing trench normal absolute upper plate velocity and slab age from 160 Myr to present at three different latitudes from Maloney et al. (2013). Please note the correlation among subduction of young oceanic floor, high trenchward upper plate motion, and the onset of slab shallowing in the analyzed Andean segments.

5. Regional arc evolution between 35°30' to 48°S: A ~1350 km large-scale flat subduction segment?

As described in the previous section, arc migration segments potentially linked to slab shallowing/flattening events are not local phenomenona. As depicted in Fig. 12a these zones are latitudinally connected forming a continuous segment ~1350 km long that can be alternatively conceived as a single arc expansion/migration process. If right, this potential process was diachronic as reflected on the ages of initial expansion of the different arc

segments (Figs. 10 and 11). In this sense, the first change in subduction angle may have taken place in the segment from 48°S to 44°30'S at ~120 Ma (Suárez et al., 2009a; Gianni et al., 2015a) (Fig. 11b). Then, this episode seems to have generalized since 100-90 Myr, propagating northward and achieving its full development during the 75-60 Myr time interval (Fig. 10 and 11). It is worth noting that diachronism in arc shifting is apparently reflected in the beginning of synorogenic deposition in the foreland, as well as, broken foreland basins related to the analyzed fold-thrust belts (Fig. 2). Nevertheless, at this time the configuration of the subduction system may have been complex as indicated by an eastwardly displaced active arc north of 40°30'S (Ramos and Folguera, 2005; Spagnuolo et al., 2012; García Morabito and Ramos, 2012) and an arc shut-off to the south (Gianni et al., 2015a; Suárez and de la Cruz, 2001) (Figs 10b, 11b and 12a). Although complex, this situation is strikingly alike to the current situation of the Chilean/Pampean flat-slab (Álvarez et al., 2015). We speculate that similarly to the latter segment, it could have been due to a slightly different slab configuration north and south of the 40°30'S latitude. A prevailing shallow angle to the north may have allowed arc magmatism production out of a preserved mantle wedge (Ramos and Folguera, 2005), whereas a flat angle to the south extruded the mantle wedge during full plate horizontalization, cancelling magmatic production (Gianni et al., 2015a; Echaurren et al., 2016a) (Fig. 12a). The potential connection among some of the Southern Central Andes shallowing/flat-slab events was initially suspected by García Morabito and Ramos (2012). The regional analysis presented in this review expands this idea and suggests the potential existence of a ~1350 km long shallow to flat-subduction segment in Late Cretaceous-Early Paleogene. This episode is here referred to as the *Nalé large flat-slab* event (Fig. 12a). It is worth noting that this episode could have been linked to a subduction segment as large as the biggest flat-slab on earth, known as the Peruvian large flat-slab that runs ~1400 km along the South American margin between 4°S to 15°S (Gutscher, 2000) (Fig. 12b). Noteworthy, such large-scale modifications in subduction settings are rare and poorly documented in the geological record. In this regard, Gutscher (2000) differentiated this type of processes from more common small-scale slab shallowings/flattenings and classified them as large flat-slab configurations. Indeed, the hypothetical Nalé event would have shared several features with other large flat-subduction events such as the Cretaceous to Paleogene Laramide event (U.S) and the current Chilean/Pampean and Peruvian flat-slabs, where orogenic stages took place in concert with arc expansions followed, by stress transmission far inland developing intraplate contractional belts (Dickinson and Snyder, 1978; Folguera and Ramos, 2011; García Morabito and Ramos 2012; Gianni et al., 2015a; Echaurren et al., 2016a). Nevertheless, intraplate

contraction is not unique to flat-subduction settings and several additional parameters (e.g., high convergence rates) may occasionally produce the same distal deformational effects (Raimondo et al., 2014). Magmatic migration/expansion distances from previous arc positions before magmatic shut-off in large flat-slab settings are variable (e.g., South Korea flat-slab, 250 km, Egawa et al. 2013, Fig. 7; Laramide flat-slab, 800 km, Coney and Reynolds, 1977; South China flat-slab, 1000 km, Li and Li, 2007, Fig. 3). Particularly, the Peru large flat-slab magmatic expansion did not surpass in average the ~250 km before magmatic shut-off (Hu and Liu, 2013) (Fig. 12c). Notably, the latter observation is comparable to arc migrations described in the *Nalé large flat-slab* (Figs. 10b and 11b). The proposed *Nalé large flat-slab* would have had a 45-40 Myr time-spam of arc migration before stabilization or magmatic quiescence, which is comparable to other large flat/shallow subduction settings (e.g., Fig. 3; South Korea flat-slab, 100 Ma, Egawa et al. 2013, Fig. 7; Laramide flat-slab, 45 Ma, Coney and Reynolds, 1977; South China flat-slab, 60 Ma, Li and Li, 2007).

A feature recently detected on large flat-slab settings is the formation of slab tears at their edges due to buoyancy contrasts producing stretching in the transitions of flat to normal (30°) subduction angles (e.g., Burd et al 2014; Antosijevic et al., 2015). Notably, a slab tear in the northernmost extreme of the Nalé large flat-slab could account for the anomalous magmatism and slab detachment inferred by Ianelli et al (2017) and Fennell et al (2017) at 35º30'S.

The origin of flat-subduction settings has been related to a wide variety of processes. The most commonly invoked driving mechanisms are: (a) the subduction of buoyant oceanic features such as oceanic plateaus and seamounts (e.g., van Hunen et al., 2002; Liu et al., 2010); (b) slab uplift due to the hydrodynamic suction force in the mantle wedge linked to the presence of a deep cratonic root (200-300 Km) (e.g., Jones et al., 2011; Manea et al., 2012). (c) slab uplift due to eastward relative mantle flow (e.g., Doglioni et al., 2007; Panza and Doglioni, 2015) (d) the rapid overriding of a continent over young oceanic lithosphere (van Hunen et al., 2000). According to Hu et al. (2016) the simultaneous action of these processes is necessary to explain active flat–subduction settings in South America.

The influence of the subduction of buoyant oceanic features on the origin of the Nalé flat-slab event cannot be disregarded. Nevertheless, assessing their role in ancient flat-subduction settings is challenging. In this sense, global plate reconstructions do not show any potential interaction of oceanic plateaus or seamount chains that could be linked to the Nalé flat-slab (e.g., Müller et al., 2016). Although not completely necessary, there is no evidence of accreted oceanic material in Cretaceous times in the Patagonian margin that would help to infer the subduction of a buoyant oceanic feature.

The lithosphere in southern South America is about 70-55 km thick (Tassara et al., 2006), which is largely inherited from continental stretching linked to the formation of the South Atlantic Ocean. Hence, the lack of a deep cratonic lithosphere in the study area and the absence of geological evidence of past existence of it precludes considering a hydrodynamic suction influence on the Nalé flat-slab. The westward drift of the lithosphere implies a relative eastward mantle flow that in the context of eastward-directed Andean subduction may have aided to develop slab shallowing. Nevertheless, additional factors are still needed to account for the full flat-slab geometry in late Cretaceous. Using global plate reconstructions Gianni et al., (2015a), Fennell et al. (2015) and Echaurren et al. (2016a), showed that subduction of young oceanic lithosphere coincided in space and time with the described arc-magmatic expansions. As shown in Fig. 12d there is a striking correlation among subduction of young oceanic floor, high trench normal absolute upper plate motion, and the onset of slab shallowing in the analyzed segments. Furthermore, the northward progression in subduction of young lithosphere explains the diachronic character of the Nalé flat-slab, which is not easily accounted by previously analyzed slab shallowing mechanisms. From a global analysis Cruciani et al. (2005) showed that there is no relation between slab age and dip, but that this correlation is better when considering the subduction rate. However, these authors did not include the absolute upper plate velocity in their analysis, which is expected to modify the slab angle when a young plate (40 Ma or less) is overridden, as indicated by analog and numerical modeling (Van huene et al., 2002, Liu and Currie, 2015). Hence, it is possible that in the context of polarized mantle flow (Doglioni et al., 2007), fast overriding of young oceanic lithosphere at these latitudes could have been the key to trigger a full flat-subduction configuration.

Termination of large-scale flat-subduction is often related to dramatic geodynamic changes in the subduction margin and intraplate areas. Two of the most common features are a trenchward retreat of the magmatic arc linked to slab steepening and massive outpouring of intraplate extensional magmatism produced by sudden asthenospheric upwelling (Humphreys et al., 1993; Li and Li, 2007). Strikingly, destabilization of the proposed *Nalé large flat-slab* would have taken place during Paleogene times following similar tectonomagmatic characteristics (Fig. 13). It was a diachronic process first achieved through the development of a slab window between 55-40 Myr that produced bimodal magmatism linked to the parallel subduction of the Alluk-Farallon mid-ocean ridge (Espinoza et al., 2005; Aragón et al., 2011). This stage was accompanied by upper plate extension as expected in these settings (see type 8 rifting, Doglioni, 1995). This process was followed by a trenchward arc expansion and further

eruption of intraplate volcanic rocks from Oligocene to early Miocene times produced by mantle upwelling triggered by slab steepening (Kay et al., 2006; Encinas et al., 2015; Folguera et al., 2015; Fernandez-Paz et al., 2017, among others) (Figs. 10b; 11b; 13). Trenchward expanded arc achieved its maximum expression in the Coastal magmatic belt (CB) and the Traiguén basin (TB) located in the current forearc region close to the Chilean trench (Muñoz et al., 2000; Encinas et al., 2015) (Fig. 13).

6. The Nalé large flat-slab event and its bearings on Maastrichtian-Danian paleogeography

In Latest Cretaceous to early Paleocene, dramatic paleogeographic changes took place in the Neuquén and Patagonian forelands. At this moment, a restricted sector of the Southern and southern Central Andes foreland was flooded by the first Atlantic-derived transgression since Gondwana breakup (Feruglio, 1949; Aguirre-Urreta et al., 2011; Olivero and Medina, 1994) (Fig. 14). South of 49°S, this transgression used a preexisting marine pathway through the Late Cretaceous foredeep of the Austral foreland basin of the Southern Andes (Fig. 14). On the other hand, between 48° to 35°S, the transgression crossed-over the Patagonian foreland forming an isolated flooded domain that occupied an extensive intraplate area with some sectors reaching as far as the Andean foothills (Aguirre Urreta et al., 2011; Scasso et al., 2012) (Fig. 14). In this sector, the transgression bordered the southern Patagonian broken foreland and entered axially through broken foreland depocenters in the northern sector forming the Paso del Sapo embayment (Scasso et al., 2012; Echaurren et al., 2016a). Maximum flooding achieved in Danian times caused interconexion among the Neuquén–Colorado, Golfo San Jorge, and Cañadón Asfalto basins as evidenced by common marine species and genera among them (Del Río and Martínez, 2014) (Fig. 2 and 14). Particularly, the ~83 Ma age obtained by Echaurren et al. (2016a) for the fluvial to estuarine deposits of the Paso del Sapo Formation suggests that that flooding may have begun locally earlier, in Campanian times. The origin of the first Atlantic-derived transgression at studied latitudes has intrigued scientist since pioneering works in Patagonia (e.g., Weaver, 1927; Feruglio, 1949).

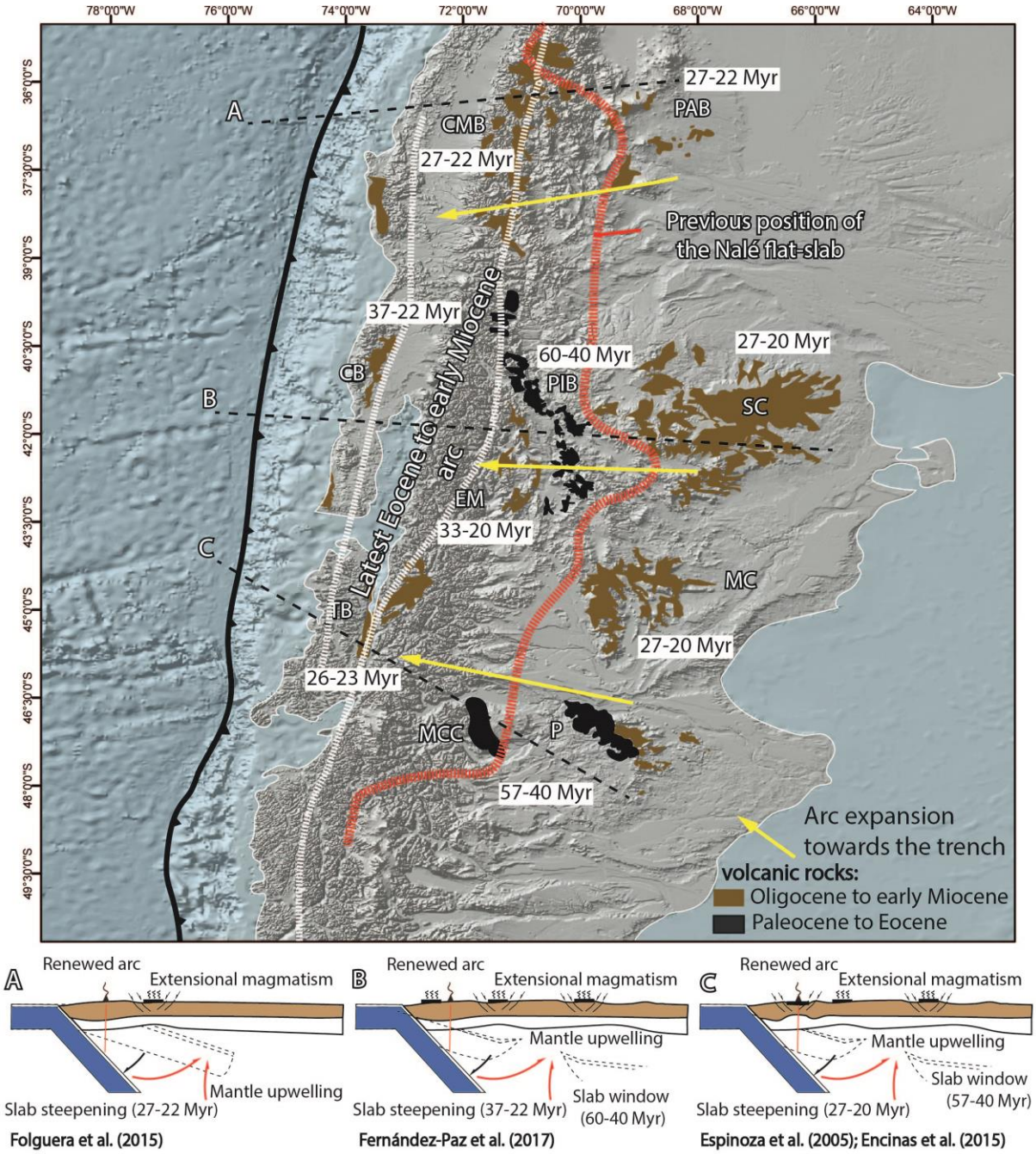

Fig. 13. Image showing the distribution of Paleogene to Neogene intraplate volcanic rocks from Patagonia. Fig. modified from Folguera and Ramos (2011) including updated geological data from Espinoza et al. (2005), Encinas et al. (2015) and Fernández-Paz et al. (2017). Below are proposed tectonic models for the Cenozoic intraplate magmatism of Patagonia at three different cross-sections. Please note the spatial coincidence between intraplate magmatism and the previous extension of the proposed Nalé large flat-slab event. Abbreviations are, P: Posadas basalts, MCC: Meseta de Chile Chico, TB: Traiguen Basin, MC: Meseta cuadrada basalts, SC: Somún Cura basalts, EM: El maiten belt, CB: Coastal magmatic belt, CMB: Cura Mallin Basin, PB: Palauco basalts, Pilcaniyeu belt.

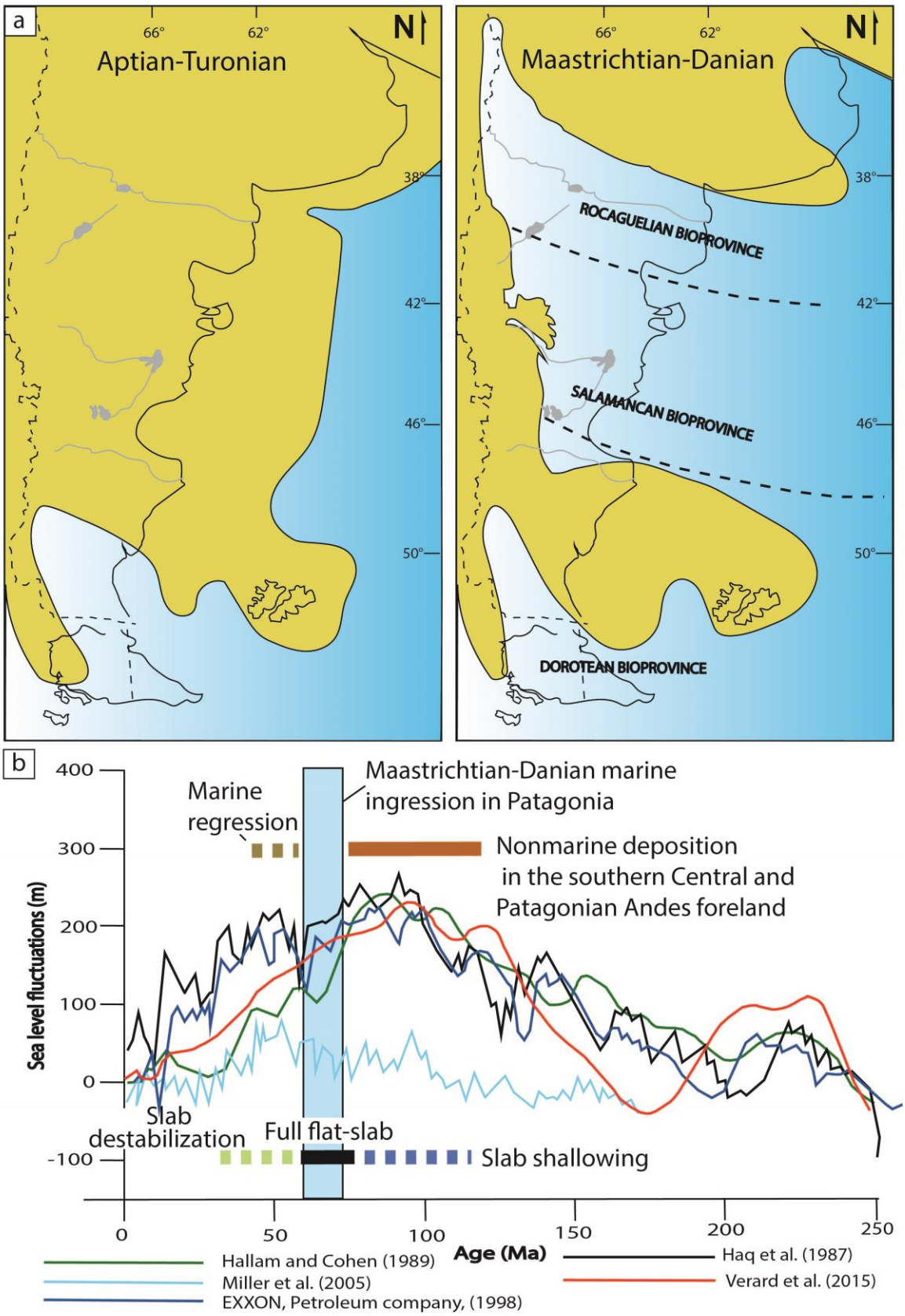

Fig. 14. a) Area covered by the Early to Late Cretaceous (modified from Spalletti and Franzese, 1996) and the Maastrichtian–Danian seas (modified from Del Río and Martínez,

2014). b) Comparison among time spams of nonmarine basin sedimentation, marine ingression and subsequent regression with various models of sea-level changes for the Phanerozoic. Please note that nonmarine deposition in the Andean basins prevailed during the periods of highest global seal level, while extensive maastrichtian-Danian marine ingression took place during a decreasing sea level. We also plotted the onset and the full development of flat subduction and the termination of this process. Please note that that the marine ingression took place at the time a full flat-slab developed and marine regression took place when this subduction geometry destabilized. Figure modified from Verard et al. (2015).

Late Cretaceous to Early Paleocene marine ingression was common to the whole Southamerican continent, especially in early Andean foredeep areas. However, Atlantic marine ingression crossing the entire platform and foreland areas from east to west was unique to Patagonia. Hence, it was rapidly acknowledged that this event could have not been solely produced by a global eustatic high in sea level at that time. The most accepted hypothesis for this enigmatic event invokes combined processes of continental tilting, produced by foreland flexure linked to Andean orogenic building, in conjunction with a global eustatic high sea level in Maastrichtian-Danian times (e.g., Nullo and Combina, 2011; Uliana and Bibble, 1988; Aguirre-Urreta et al., 2011). However, as seen from global curves of sea level variations in Fig. 14b, nonmarine deposition in the southern Central and Patagonian foreland zones prevailed during the periods of highest global sea level. Conversely, the extensive Maastrichtian-Danian marine ingression took place when the sea level was decreasing (Haq et al., 1987; Hallam and Cohen, 1989; EXXON, 1998; Miller et al., 2005; Verard et al., 2015). Additionally, according to some of these studies marine regression in the study area would have taken place during a transient increase in global sea level (Haq et al., 1987; Hallam and Cohen, 1989; EXXON, 1998; Miller et al., 2005) (Fig. 14b). The latter observations highlight the limitations of invoking an origin related to sea level fluctuations for the Patagonian marine flooding in latest Cretaceous-Paleocene times. Furthermore, an attenuated foreland lithosphere (70-55 km), remnant of South Atlantic ocean opening, is not be consistent with surfaces at sea level but rather with continental exhumed surfaces (Dávila et al., 2018). In order to analyze the influence of orogenic load on continental tilting, we calculated flexure profiles on the central region of the analyzed area (Fig. 15a), based on a balanced cross-section from Echaurren et al. (2016) (see Fig. 5d), which is the most detailed section available. This cross-section covers the eastern sector of the North Patagonian Andes and the totality of the broken foreland area, whose proximal loads are expected to have a maximum influence in the flexural subsidence (Garcia-Castellanos et al., 2002). The tectonic

topography that mostly resulted from the Cretaceous shortening event is used to account for the loads during the broken foreland formation. Hence, for this analysis we use this cross-section, and its estimation of crustal shortening, and the geometry of the orogenic load (Fig. 15a). The load-related flexure depends on the effective elastic thickness (Te), a proxy of long-term lithospheric rigidity, in addition to other rheological parameters (e.g., Watts, 2001). In our estimation a Te value of 30 km was used for the study area following the regional Te analysis of Pérez-Gussinyé et al. (2009). This analysis shows that the accommodation space next to the load (~2.5 km) is restricted in terms of wave-length, diminishing within about 150-130 km (Fig. 15a). Noteworthy, the implementation of lower Te values in our flexure analysis, as those calculated by Gianni et al. (2017) (~10 km) in the area, would yield an even smaller wave-length. Although, this factor may have contributed to continental tilting, it fails to explain the long wave-length subsidence far from the Andean orogenic load needed to allow flooding of the foreland region in a context of global sea level decrease. Hence, in the complex Cretaceous-Paleocene tectonic context discussed in this work, additional factors may have been involved in the processes that drove marine flooding of the Patagonian interior. An alternative mechanism to induce this process is dynamic subsidence, which is much broader and flatter than tectonically driven flexure (Eakin et al., 2014). Dynamic topography is linked to lithospheric deflections that are supported dynamically by mantle flow related to plume-upwelling or downwelling produced by subduction (e.g., Olson and Nam, 1986; Hager, 1984; Mitrovica et al., 1989). Recent studies have shown that subduction-related dynamic topography is very sensitive to slab geometry, particularly flat-subduction settings (Dávila et al., 2010). This particular slab configuration produce forelandward shifting of subduction-related dynamic subsidence focus linked to continental downwarping where the slab resumes it descent into the mantle (Dávila et al., 2010; Eakin et al., 2014). Subsequently, we analyze the contribution of the hypothetical *Nalé large flat-slab* during its full development in Maastrichtian-Danian times to dynamic topography in Central Patagonia. Since the most likely explanation for this flat-slab event involved the subduction of young and hotter slabs, we followed the same approach of Eakin et al. (2014) that utilizes a low density contrast to produce subducted slab flattening due to buoyant subducted plates.

Since we do not know the exact slab morphology of the *Nalé large flat-slab*, a simplification in our approach is that we used a 1350 km long subhorizontal plate with a similar morphology to the Peru flat-slab (Eakin et al., 2014). The main parameters affecting the instantaneous dynamic topography model (see Hager and O'Connel, 1979; for further details) are the density contrast and subduction geometry between the slab and the asthenospheric mantle.

High positive density contrast produces large dynamic subsidence; low or neutral contrasts, in opposition, drive no dynamic topography. In the models of Dávila et al. (2010) and Eakin et al. (2014) flat-slabs show the lowest density contrast across the buoyant area. Flat-slab configurations change the density contrasts toward its leading edge to more positive values, where subduction becomes steeper and dynamic subsidence takes place. Therefore, the larger a flat slab is, the more distant dynamic subsidence occurs. Density anomalies (relative to background mantle, up to 80 kg/m^3) were assigned to the slab model following the plate kinematic model of Müller et al. (2016) using subducting plate age at the trench at 70 Ma. For the segment where the slab is horizontal, the density anomaly was set to zero ($\delta\rho$=0 kg/m3) to simulate neutral buoyancy. This particular density structure is suitable for slab flattening caused by subduction of young slabs or subducting buoyancy features like an oceanic plateau (Appendix in Dávila and Lithgow-Bertelloni, 2015). In addition to a flat-slab scenario, we elaborate a slab model for normal subduction (30◦E) in order to represent how subduction and related dynamic topography looked prior to the onset of flat-subduction. The latter was achieved by solving the equations for the conservation of mass and momentum using propagator matrices in a spherical shell (Hager, 1984; Hager and O'Connell, 1979, 1981). Density and flow fields are computed to spherical harmonic degree and order 50 (plotted to degree 40). A Newtonian mantle rheology and a viscosity varying with radius were assumed. A Non-Newtonian rheology is not considered in this model which may modify dynamic subsidence in areas close the trench. However, as in this study we mainly focus in flat-subduction affecting distal foreland areas, we do not expect significant variations in the obtained results of dynamic subsidence (Zhong and Gurnis, 1994).

The calculated dynamic topography at a given time is independent of the absolute viscosity but the amplitude does depend on the relative viscosity contrast between each layer. The viscosity contrasts between the modeled layers (lithosphere, upper and lower mantle) affect very little, and more particularly on the amplitude rather than wavelength of dynamic subsidence. Results are presented for a viscosity structure of 10 for the lithosphere (120 km thick) and 50 for the lower mantle, as normalized to the upper mantle, based on the best correlation with the geoid and which is consistent with previous studies (Lithgow-Bertelloni and Gurnis, 1997; Dávila et al., 2010). In this viscosity structure the lithosphere is 10 times more viscous than the upper mantle, indicative of a mobile lithosphere, the asthenosphere is 10 times less viscous than the upper mantle and the lower mantle is 50 times more viscous than the upper mantle. We kept the viscosity structure constant throughout. Using this mantle viscosity structure the dynamic topographies predicted by each of the slab models are shown

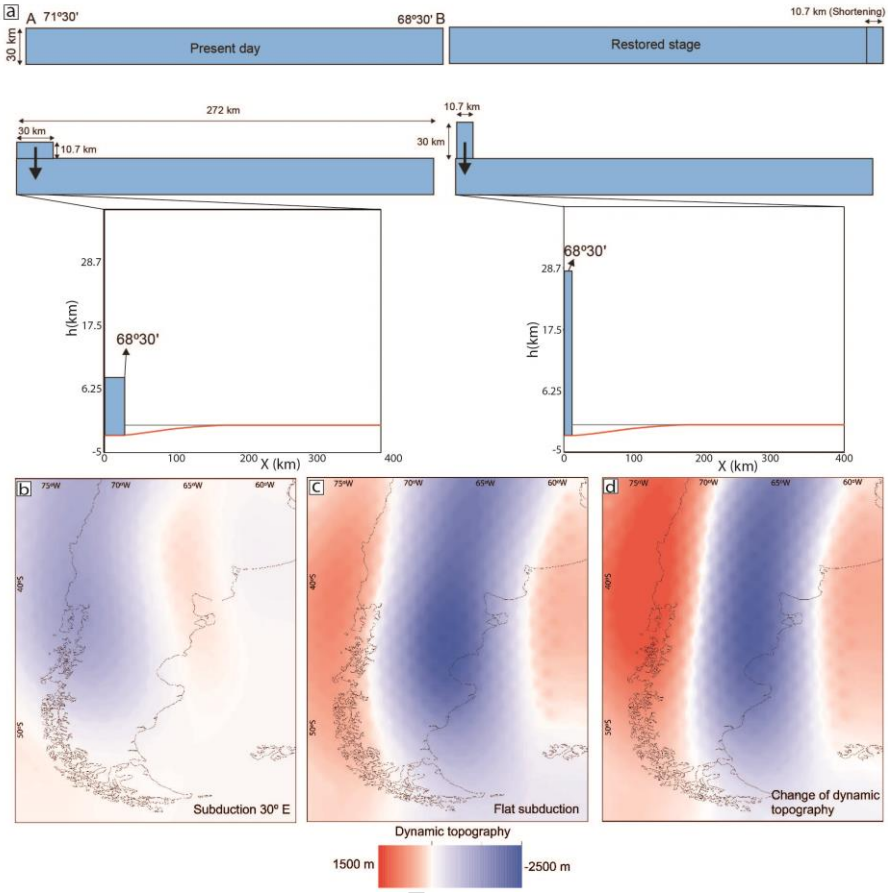

Fig. 15. a) Flexural curves (two red lines) calculated based on loading a charge with two different distributions. The load was calculated and reconstructed from the extent of crustal shortening estimated from a balanced cross-section at 43°S (Echaurren et al., 2016a) and using an elastic thicknesses of 30 km (Te) (Pérez-Gussinyé et al., 2009). Below is a comparison of dynamic topography shown in 2D predicted by two different slab models b) a normal angle (30ºE) subduction, previous to flat-subduction onset, and c) for Nalé large flat-slab full development in Maastrichtian-Danian times. d) Change in dynamic topography from stage b) to c).

in Fig. 15b-c-d. For the normal subduction stage, the model predicts dynamic subsidence underneath the Chile trench and over the Andes (Fig. 15b). Contrastingly, in the flat-slab model, dynamic subsidence of long-wavelength (~1300 km) and an amplitude of >1 km, is displaced to the east in the Southern Central and Southern Andean foreland (Fig. 15c), which is in harmony with previous findings of Eakin et al. (2014) for the Peru flat-slab. An outcome in the presented models, originally noticed and analyzed in previous works (e.g., Dávila and Lithgow-Bertelloni, 2013; Eakin et al., 2014), is that the transition from normal to flat subduction would predict transient relative dynamic uplift along the Andes but relative

dynamic subsidence in the distal Patagonian foreland (Fig. 15d). These positive values, however, do not denote a positive contribution on the topography, but rather they imply positive vertical displacements with respect to the previous stage, because the dynamic negative support is reduced or eliminated (Dávila and Lithgow-Bertollini, 2013). Noteworthy, it is a result of the model used which is based on the assumed process responsible for slab flattening in the study area. Contrarily, dynamic subsidence may be expected above the flat-slab on other scenarios as described for the Laramide subduction (Liu et al., 2010; Heller and Liu, 2016). Strikingly, dynamic foreland subsidence related to the proposed *Nalé large flat-slab* had a probable position spatially coincident with the flooded continental zone discussed in this study (Fig. 16).

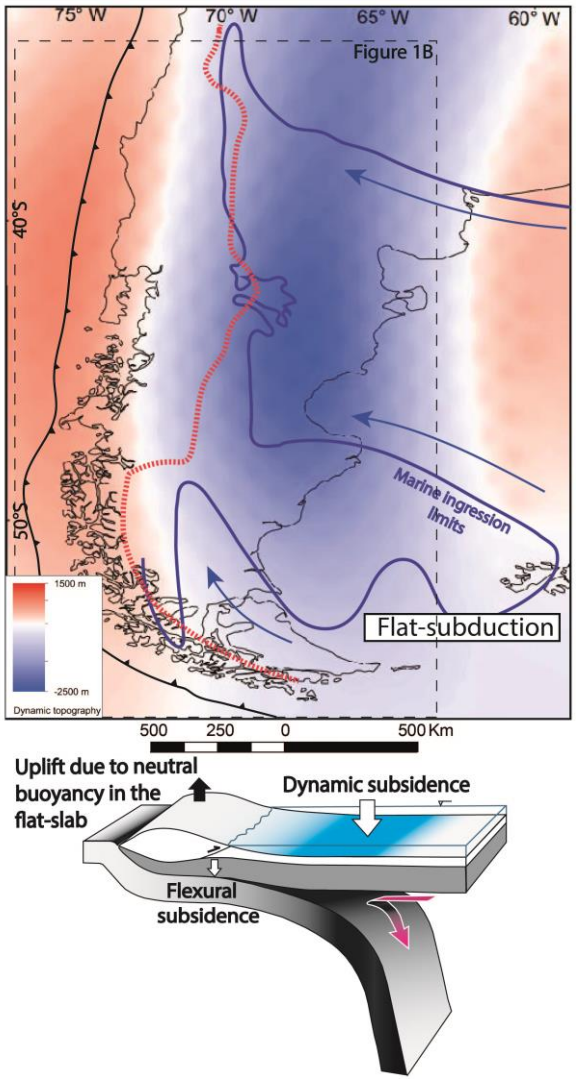

Fig. 16. Proposed model linking Late Cretaceous/Paleocene Atlantic marine ingression in Patagonia to the Nalé large flat-slab. In this model, the ingression was produced by continental tilting driven by eastward shifted dynamic subsidence in the intraplate area and uplift due to neutral buoyancy in the flat-slab portion**.** Red dashed line shows the area where

the arc expanded abnormally in relation to the hypothetical Nalé large flat-slab. Scheme below is modified from Heller and Liu (2016).

We suggest that this process along with a predicted change of ~1-0.8 km of vertical motion near the plate margin (Fig. 15d) along the ~1350 km flat-slab segment may have played a key role on the classically invoked latest Cretaceous-early Paleocene continental tilting. Moreover, it may elegantly explain the restricted character of the flooded area, which is evident from the distribution of paleoshore lines that coincided with the latitudes where the hypothetical *Nalé large flat-slab* would have developed (Fig. 16). Therefore, subtle continental tilting directly linked to the *Nalé large flat-slab event* may have driven sudden paleogeographic changes allowing a marine ingression in the Southern Central and Southern Andean foreland during a decreasing eustatic sea level stage in Maastrichtian-Danian times (Fig.16). Noteworthy, termination of flat-subduction and hence, distal dynamic subsidence may explain the late Paleocene marine regression in the study area, which paradoxically took place during increasing sea global levels according to most studies (Haq et al., 1987; Hallam and Cohen, 1989; EXXON, 1998; Miller et al., 2005) (Fig. 14b).

Similarly, the Western Interior Seaway which covered much of western North America until ~70 Ma has been interpreted as related to dynamic subsidence at the edge of the Laramide flat-slab (e.g., Cross and Pilger, 1978; Mitrovica et al., 1989; Heller and Liu, 2016).

7. Conclusions

A synthesis of most recent tectonic studies of the Andes between 35°30' to 48°S presented in this work highlights the regional character of Cretaceous contraction. Initial orogenic building phases defined early growth stages in the Malargüe, Chos Malal, Agrio, Aluminé, and North Patagonian fold-thrust belts. Notably, part of the Cretaceous shortening was absorbed far from the plate margin in the intraplate sector, giving place to an early expression of the Cenozoic Patagonian broken foreland. Most of the analyzed works identified a spatio-temporal relation between magmatic arc migrations or expansions, and fold-thrust belt development. An analysis of arc magmatism during these orogenic building stages revealed a 400-520 km arc migration from trench of diachronic character, beginning at 120 Ma between 48ºS to 44º30'S and propagating northward since 100-90 Myr up to 36ºS. This process was followed by a 20-10 Myr magmatic shut-off that affected a large segment of the previous expanded arc between 48ºS to 40º30'S. From the analysis of the main processes controlling arc dynamics, changes in slab dip related to slab swallowing seem to be the most likely cause for the observed arc

evolution.

Alternatively to previous works Inferring distinct subduction segments undergoing slab shallowing or flattening events, the analysis presented in this contribution opens the possibility of the existence of a single process linked to a potential ~1350 km long flat-slab. We referred to this hypothetical stage as the *Nalé large flat-slab event*. This process could have initiated in late Early Cretaceous and achieved full development in latest Cretaceous to earliest Paleocene times. Noteworthy, diachronism in the slab shallowing process was mirrored by a northward younging trend in synorogenic deposition in foreland and broken foreland basins related to the analyzed fold-thrust belts. The potential dimensions of this event allow us to classify it as a large flat-slab segment which could have been as long as the Peruvian flat-slab, the largest subhorizontal subduction configuration on earth. In the potential context of relative eastward mantle flow, the east-directed Andean subduction along with fast overriding of young oceanic lithosphere could have triggered the Nalé flat-slab in Late Cretaceous times. As documented in similar flat-slab settings, destabilization of the *Nalé large flat-slab event* could also explain the massive outpouring of synextensional intraplate volcanic rocks in Patagonia and the arc retraction in mid-Paleogene to early Neogene times. Additionally, the combination of load-related orogenic flexure during sea level fluctuations often invoked to explain foreland marine flooding in Maastrichtian-Danian times may have been significantly aided by the *Nalé large flat-slab,* as these settings are expected to cause dynamic vertical motion of the continental margin and subsidence in the foreland area. It is worth to remember that in a foreland region, far from the major tectonic loads, no many other subsidence mechanisms allow reproducing such a regional sinking. An origin for this marine ingression directly linked to sea level fluctuations is disregarded because contrary to as expected, marine flooding took place during a decreasing global sea level stage. Similarly, it is possible that the late Paleocene marine regression could have taken place during a transient increase in sea level according to most studies. In this study, we link both, marine ingression and regression, to the evolution of the Nalé flat-slab event based on the close time-space relation with the onset of a fully developed slab flattening and the termination of this process. Testing the feasibility of this proposal will require additional constraints on the geochronology and geochemistry of arc rocks along the 36°S-48°S arc segment. An alternative future work might be to invert seismic tomography to reconstruct the Cretaceous subduction scenarios using an adjoint method (e.g., Liu et al., 2008). Finally, this review underscores pre-Cenozoic contractional stages in Andean evolution and the importance of slab shallowing or flattening as an effective driving process for subduction orogenesis.

6. Acknowledgement

The authors want to recognize the support received by CONICET and the many lively discussion with several members of the Laboratorio de Tectónica Andina and the Instituto Sismológico Ing. Fernando Volponi (IGSV) through the years. FMD thanks PUE 2016-CICTERRA, SECyT-UNC, and FONCYT. Constructive comments from Marco Bonini, an anonymous reviewer and Editor Carlo Doglioni are greatly appreciated. We are grateful to Brian Horton, Victor Ramos and Kevin Ward for suggestions that substantially improved an early version of this manuscript.

7. References

Adriasola, A.C., Thomson, S.N., Brix, M.R., Hervé, F., Stöckhert, B., 2006. Postmagmatic cooling and late Cenozoic denudation of the North Patagonian Batholith in the Los Lagos region of Chile, 41°-42°15′S. Int. J. Earth. Sci. 95(3): 504-528

Aguirre-Urreta, B., Ramos., V.A., 1981. Estratigrafía y paleontología de la alta cuenca de río Roble, Cordillera Patagónica. In: VIII Congreso Geológico Argentino. Actas III. pp 101–138

Aguirre-Urreta, B., Tunik, M., Naipauer, M., Pazos, P., Ottone, E., Fanning, M., Ramos, V. A., 2011 Malargüe Group (Maastrichtian–Danian) deposits in the Neuquén Andes, Argentina: Implications for the onset of the first Atlantic transgression related to Western Gondwana break-up. Gond. Res. 19(2), 482-494

Antonijevic, S.K., Wagner, L.S., Kumar, A., Beck, S.L., Long, M.D., Zandt, G., Tavera, H., Condori, C., 2015. The role of ridges in the formation and longevity of flat slabs. Nature, 524, 212–215.

Allard, J.O., Foix, N., Rodríguez, A., Sánchez, F., 2015. Evolución tectosedimentaria de la cuenca del golfo San Jorge en su margen occidental. Reunión de Tectónica (Río Negro). Electronic book

Álvarez, O., Giménez, M., Folguera, A., Spagnotto, S., Bustos, E., Baez, W., Braitenberg, C., 2015. New evidence about the subduction of the Copiapó ridge beneath South America, and its connection with the Chilean-Pampean flat slab, tracked by satellite GOCE and EGM2008 models. J. Geod. 91, 65-88

Álvarez Cerimedo., J., Orts, D., Rojas Vera, E., Folguera, A., Bottesi, G., Ramos, V.A., 2013. Mecanismos y fases de construcción orogénicos del frente oriental andino (36 S, Argentina). And. Geol. 40(3), 504-520.

Aragón, E., D' Eramo, F., Castro, A., Pinotti, L., Brunelli, D., Rabbia, O., Rivalenti, G.,Varela, R., Spakman,W., Demartis M, Cavarozzi C, Aguilera Y, Mazzucchelli M, Ribot A., 2011. Tectono-magmatic response to major convergence changes in the North Patagonian suprasubduction system; the Paleogene subduction–transcurrent plate margin transition. Tectonophysics, 509, 218–237

Armijo, R., Lacassin, R., Coudurier-Curveur, A., Carrizo, D., 2015. Coupled tectonic evolution of Andean orogeny and global climate. Earth-Sci. Rev. 143, 1-35

Arriagada, C., Cobbold, P.R., Roperch, P., 2006. Salar de Atacama basin: A record of compressional tectonics in the central Andes since the mid-Cretaceous. Tectonics, 25(1).

Baker, P.A., Fritz, S.C., Dick, C.W., Eckert, A.J., Horton, B.K., Manzoni, S., Battisti, D.S., 2014. The emerging field of geogenomics: constraining geological problems with genetic data. Earth-Sci. Rev. 135, 38-47.

Balgord, E.A., Carrapa, B., 2016. Basin evolution of Upper Cretaceous–Lower Cenozoic strata in the Malargüe fold-and-thrust belt: northern Neuquén Basin, Argentina. Bas. Res. 28(2), 183-206.

Barcat, C., Cortiñaz, J.S., Nevistic, V.A., Zucchi, H.E., 1989. Cuenca Golfo San Jorge. In: Chebli, L.S. (Ed.) Cuencas Sedimentarias Argentinas, Serie Correlación Geológica 6 Tucumán, pp 319–345

Barnes, J.B., Ehlers, T.A., 2009. End member models for Andean Plateau uplift. Earth-Sci. Rev. 97:(1–4)105–132 http://dx.doi.org/10.1016/j.earscirev.2009.08.003.

Bilmes, A., D'Elia, L., Franzese, J.R., Veiga, G.D., Hernández, M., 2013. Miocene block uplift and basin formation in the Patagonian foreland: The Gastre Basin, Argentina. Tectonophysics, 601: 98–111

Boll, A., Alonso, J., Fuentes, F., Vergara, M., Laffitte, G., Villar, H.J., 2014. Factores controlantes de las acumulaciones de hidrocarburos en el sector norte de la cuenca neuquina, entre los ríos Diamante y Salado, provincia de Mendoza, Argentina. In: Actas del IX Congreso de Exploración y Desarrollo de Hidrocarburos: trabajos técnicos 1, 3-44.

Burd, A.I., Booker, J.R., Mackie, R., Pomposiello, C., Favetto, A., 2013. Electrical conductivity of the Pampean shallow subduction region of Argentina near 33 S: evidence for a slab window. Geochem. Geophys. Geosyst. 14 (8), 3192–3209.

Castro, A., Moreno-Ventas, I., Fernández, C., Vujovich, G., Gallastegui, G., Heredia, N., Martino, R.D., Becchio, R., Corretgé, L.G., Díaz-Alvarado, J., Such, P., García-Arias, M., Liu, D.Y., 2011. Petrology and SHRIMP U-Pb zircon geochronology of Cordilleran granitoids of the Bariloche area, Argentina. J. S. Am. Earth. Sci. 32(4), 508-530

Cazau, L., Uliana, M., 1973. El Cretácico Superior continental de la Cuenca Neuquina. V Congreso Geológico Argentino, Actas (Córdoba, Argentina) 3:131–163

Cazau, L., Mancini, D., Cangini, J., Spalletti, L., 1989. Cuenca de Ñirihuau. In: Chebli, G., Spalletti, L., (Eds.) Cuencas Sedimentarias Argentinas, Serie Correlación Geológica 6:299-318, Tucumán.

Césari, S.N., Limarino, C.O., Llorens, M., Passalia, M.G., Loinaze, V.P., Vera, E.I., 2011. High-precision late Aptian Pb/U age for the Punta del Barco Formation (Baqueró Group), Santa Cruz Province, Argentina. J. S. Am. Earth. Sci. 31, 426–431

Charrier, R., Pinto, L., Rodriguez, M., 2007. Tectonostratigraphic evolution of the Andean orogen in Chile. In Moreno, T., Gibbons W. (Eds.), The Geology of Chile, Geol. Soc. Lond., p. 21–114.

Clavijo, R., 1986. Estratigrafía del Cretácico Inferior en el sector occidental de la Cuenca del Golfo San Jorge. Boletín Inf. Pet. 9, 15–32

Cobbold, P.R., Rosello, E.A., 2003. Aptian to recent compressional deformation, foothills of the Neuquén Basin, Argentina. Mar. Petrol. Geol. 20:429-443.

Coney, P,J., Reynolds, S.J., 1977. Cordilleran benioff zones. Nature, 270(5636), 403.

Continanzia, J., Manceda, R., Covellone, G.M., Gavarrino, A.S., 2011. Cuencas de Rawson y Valdés : Síntesis del Conocimiento Exploratorio – Visión actual. In: Kozlowski, E., Legarreta, L., Boll, A., Marshall, P.A. (Eds), Simposio Cuencas Argentinas Visión Actual: VIII Congreso de Exploración y Desarrollo de Hidrocarburos pp 47–64

Cross, T.A., Pilger. Jr. R.H., 1978. Tectonic controls of Late Cretaceous sedimentation, western interior, USA. Nature, 274, 653–657. http://dx.doi.org/10.1038/274653a0.

Eakin, C.M., Lithgow-Bertelloni, C., Dávila, F.M., 2014. Influence of Peruvian flat-subduction dynamics on the evolution of western Amazonia. Earth. Planet. Sci. Let. 404, 250-260.

Egawa, K., 2013. East Asia-Wide Flat Slab Subduction and Jurassic Synorogenic Basin Evolution in West Korea. In Mechanism of Sedimentary Basin Formation-Multidisciplinary Approach on Active Plate Margins. InTech.

Encinas, A., Folguera, A., Oliveros, V., De Girolamo Del Mauro, L., Tapia, F., Riffo, R., Hervé, F., Finger, K.L., Valencia, V.A., Gianni, G.M., Álvarez, O., 2015. Late Oligocene–Early Miocene submarine volcanism and deep marine sedimentation in an extensional basin of southern Chile: implications on the tectonic development of the North Patagonian Andes. Geol. Soc. Am. Bull. 128(5-6), 807-823.

Espinoza, F., Morata, D., Pelleter, E., Maury, R.C., Suárez, M., Lagabrielle, Y., Polvé, M., Bellon, H., Cotton, J., De la Cruz, R., Guivel, C., 2005. Petrogenesis of the Eocene and MioPliocene alkaline basaltic magmatism in Meseta Chile Chico, southern Patagonia, Chile: evidence for the participation of two slab windows. Lithos, 82, 315–343.

Dalziel, I.W.D., deWit, M.J., Palmer, K.F., 1974. Fossil marginal basin in the Southern Andes. Nature, 250:291–94

Dávila, F., Lithgow-Bertelloni, C., Giménez, M., 2010. Tectonic and dynamic controls on the topography and subsidence of the Argentine Pampas: The role of the flat slab. Earth. Planet. Sci. Let. 295(1), 187-194

Dávila, F., Lithgow-Bertelloni, C., 2013. Dynamic topography in South America. J. South Am. Earth Sci. 43, 127–144.

Dávila, F. M., Lithgow-Bertelloni, C., 2015. Dynamic uplift during slab flattening. Earth Planet. Sci. Let. 425, 34-43.

Dávila, F. M., Lithgow-Bertelloni, C., Martina, F., Ávila, P., Nóbile, J., Collo, G, et al. (2018). Mantle Influence on Andean and Pre-Andean Topography. In Folguera et al. (Eds.), The Evolution of the Chilean-Argentinean Andes (pp. 363-385). Springer, Cham.

Demant, A., Suárez, M., 2007. Geochronology and petrochemistry of Late Cretaceous- (?) Paleogene volcanic sequences from the eastern central Patagonian Cordillera (45° -45º40' S). Rev. Geol. Chile. 34, 3–21

del Río, C.J., Martínez, S.A., 2015. Paleobiogeography of the Danian molluscan assemblages of Patagonia (Argentina). Palaeog. Palaeoc. Palaeoec. 417, 274-292.

Di Giulio, A., Ronchi, A., Sanfilippo, A., Tiepolo, M., Pimentel, M., Ramos, V.A. 2012. Detrital zircon provenance from the Neuquén Basin (south-central Andes): Cretaceous geodynamic evolution and sedimentary response in a retroarc-foreland basin. Geology, 40:559-562.

Di Giulio, A., Ronchi, A., Sanfilippo, A., Balgord, E.A., Carrapa, B., Ramos, V.A., 2016. Cretaceous evolution of the Andean margin between 36° S and 40° S latitude through a multi-proxy provenance analysis of Neuquén Basin strata (Argentina). Bas. Res., doi: 10.1111/bre.12176

Dickinson, W.R., Snyder, W.S., 1978. Plate tectonics of the Laramide orogeny. Geol. Soc. Am. Mem., 151, 355-366

Doglioni, C., 1995. Geological remarks on the relationships between extension and convergent geodynamic settings. Tectonophysics, 252(1-4), 253-267.

Domínguez, E., Aliotta, G., Garrido, M., Daniela, J.C., Ronconi, N., Casé, A.M., Palacios, M., 1984. Los Maitenes-El Salvaje. Un sistema hidrotermal tipo porfírico. IX Congreso Geológico Argentino (Bariloche), Actas VII, 443-458.

Doglioni, C., Carminati, E., Cuffaro, M., Scrocca, D., 2007. Subduction kinematics and dynamic constraints. Earth-Sci. Rev. 83, 125-175, doi:10.1016/j.earscirev.2007.04.001.

Doglioni, C., Panza, G., 2015. Polarized plate tectonics. In Advances in Geophysics (Vol. 56, pp. 1-167). Elsevier.

Duerto, L., Escalona, A., Mann, P., 2006. Deep structure of the Mérida Andes and Sierra de Perijá mountain fronts, Maracaibo Basin, Venezuela, AAPG Bull. 90 (4), 505–528. doi:10.1306/10080505033.

Duhart, P., Adriasola, A.C., 2008. New time-constraints on provenance, metamorphism and exhumation of the Bahía Mansa Metamorphic Complex on the Main Chiloé Island, south-central Chile. Rev. Geol. Chile 35, 79–104

Echaurren, A., Folguera, A., Gianni, G., Orts, D., Tassara, A., Encinas, A., Giménez, M., Valencia, V. 2016a. Tectonic evolution of the North Patagonian Andes (41°–44° S) through recognition of syntectonic strata. Tectonophysics, 677, 99-114

Echaurren, A., Oliveros, V., Folguera, A., Ibarra, F., Creixell, C., Lucassen, F., 2016b. Early andean tectonomagmatic stages in North Patagonia: Insights from field and geochemical data. J. Geol. Soc. Lon. 10.1144/jgs2016-087

England, P., Engdahl, R., Thatcher, W, 2004. Systematic variation in the depths of slabs beneath arc volcanoes. Geoph. J. Int. 156(2), 377-408.

England, P.C., Katz, R.F. 2010. Global systematics of arc volcano position. Nature, 468(7325), E6-E7.

EXXON Petroleum Company, 1988. The EXXON 'global' sea-level curve; unpublished.

Faccenna, C., Becker, T.W., Conrad, C.P., Husson, L., 2013. Mountain building and mantle dynamics. Tectonics, 32 (1), 80–93. http://dx.doi.org/10.1029/2012tc003176.

Fennell, L.M., Folguera, A., Naipauer, M., Gianni, G., Rojas Vera, E.A., Bottesi, G., Ramos, V.A., 2015. Cretaceous deformation of the Southern Central Andes: synorogenic growth strata in the Neuquén Group (35º 30′–37º S). Bas. Res. DOI: 10.1111/bre.12135

Fennell, L., Iannelli, S.B., Folguera, A., Encinas, A., Sagripanti, L., Colavitto, B., Valencia, V., 2017. Interrupciones extensionales en el desarrollo de la Faja Plegada y Corrida de Malargüe (36°S). XX Congreso Geológico Argentino, San Miguel de Tucumán, Digital Abstracts vol. S12, pp. 88-90.

Feruglio, E., 1949. Descripción Geológica de la Patagonia. Dirección General de Yacimientos Petrolíferos Fiscales, Editorial Coni, 334

Fernández Paz, L.F., Litvak. V.D., Echaurren, A., Iannelli, S.B., Encinas, A., Folguera, A., Valencia, V., 2018. Late Eocene volcanism in North Patagonia (42° 30′ -43° S): Arc resumption after a stage of within-plate magmatism. J. Geod. 113, 13-31.

Figari, E.G., 2005. Evolución tectónica de la Cuenca de Cañadón Asfalto (Zona del valle medio del Río Chubut) Doctoral Thesis Universidad de Buenos Aires

Fildani, A., Cope, T.D., Graham, S.A., Wooden, J.L., 2003. Initiation of the Magallanes foreland basin: timing of the southernmost Patagonian Andes orogeny revised by detrital zircon provenance analysis. Geology, 31,1081–1084.

Fitzgerald, M.G., Mitchum, R.M. Jr., Uliana, M.A., Biddle, K.T., 1990. Evolution ofthe San Jorge Basin, Argentina. Am. Assoc. Pet. Geol. Bull. 74, 879–920

Folguera, A., Iannizzotto, N.F., 2004. The lagos La Plata and Fontana fold-and-thrust belt: long-lived orogenesis at the edge of western Patagonia. J. South Am. Earth. Sci. 16, 541–566

Folguera, A., Ramos, V.A., 2011. Repeated eastward shifts of arc magmatism in the Southern Andes: a revision to the long-term, pattern of Andean uplift and magmatism. J. South Am. Earth Sci. doi:10.1016/j.jsames.2011.04.003.

Folguera, A., Bottesi, G., Duddy, I., Martín-González, F., Orts, D., Sagripanti, L., Rojas Vera E.A., Ramos, V.A., 2015. Exhumation of the Neuquén Basin in the southern Central Andes (Malargüe fold-thrust belt) from field data and low-temperature thermochronology. J. South Am. Earth. Sci. 64, 381-398.

Franchi, M.R., Page, R., 1980. Los basaltos cretácicos y la evolución magmática del Chubut occidental. Rev. Asoc. Geol. Argent. 35, 208–229.

Franchini, M., López-Escobar, L., Schalamuk, I.B.A., Meinert, L., 2003. Magmatic characteristics of the Paleocene Cerro Nevazón region and other Cretaceous to Early Tertiary calalcaline subvolcanic to plutonio units in the Neuquén Andes, Argentina. J. South Am. Earth Sci. 16, 399-421

Garcia-Castellanos, D., Fernandez, M., Torné, M., 2002. Modeling the evolution of the Guadalquivir foreland basin (southern Spain). Tectonics, 21 (3). http://dx.doi.org/10.1029/2001TC001339

García Morabito, E., Ramos, V.A., 2012. Andean evolution of the Aluminé fold-thrust belt, Northern Patagonian Andes (38°300–40°300S). J. S. Am. Earth Sci. 38, 13–30

Garrido, A.C., 2010. Estratigrafía del Grupo Neuquén, Cretácico Superior de la Cuenca Neuquina (Argentina): nueva propuesta de ordenamiento litoestratigráfico. Rev. Mus. Argentino Cienc. Na.t 12(2), 121-177

Garzione, C. N., Molnar, P., Libarkin, J. C., MacFadden, B. J., 2006. Rapid late Miocene rise of the Bolivian Altiplano: Evidence for removal of mantle lithosphere. E. Planet. Sci. Let. 241(3), 543-556

Galarza, B.J., Zamora Valcarce, G., Folguera, A., Bottesi, G.L., 2009. Geología y Evolución tectónica del Frente Cordillerano a los 36º30'S: bloques de Yihuin-Huaca y Puntilla de Huincán. Mendoza. Rev. As. Geol. Arg. 65 (1), 170-191.

Ghiara, M.R., Haller, M.J., Stanzione, D., Barbieri, M., Menditti, I., Castorina, F., Trudu, C., Demichelis, A.H., Meister, C.M., 1999. Calc-alkaline volcanic rocks from Cerro Ver, Patagonian Cordillera (43º10´S): geochemistry and geochronology. XIV Congreso Geológico Argentino, Salta 2: 178-181

Giacosa, R.E., Afonso, J.C., Heredia, C.N., Paredes, J., 2005. Tertiary tectonics of the sub-Andean region of the North Patagonian Andes, southern central Andes of Argentina (41–42 30′ S). J. S. Am. Earth Sci. 20, 157–170

Giacosa, R., Zubia, M., Sánchez, M., Allard, J., 2010. Meso-Cenozoic tectonics of the southern Patagonian foreland: Structural evolution and implications for Au–Ag veins in the eastern Deseado Region (Santa Cruz, Argentina). J. S. Am. Earth Sci. 30, 134–150

Ghiglione, M.C., Naipauer, M., Sue, C., Barberón, V., Blampied, J.N., Ronda, G., Ramos, V.A., Aguirre Urreta, B.A., Valencia. V., 2013. Early Cretaceous (Aptian) uplift of Patagonia recorded on zircons detrital content from the northern Austral-Magallanes basin. In: Int. Geol. Congress South Hemisph, Viña del Mar, pp 64–66

Giambiagi, L., Bechis, F., Garcia. V., Clark, A.H., 2008 Temporal and spatial relationships of thick- and thin-skinned deformation: A case study from the Malargüe fold-and-thrust belt, southern Central Andes. Tectonophysics, 459, 123-139

Gianni, G.M., Navarrete, C., Orts, D., Tobal, J., Folguera, A., Giménez, M., 2015a. Patagonian broken foreland and related synorogenic rifting: The origin of the Chubut Group Basin. Tectonophysics, 649, 81–99. doi:10.1016/j.tecto.2015.03.006.

Gianni, G.M., Navarrete, C.G., Folguera, A., 2015b. Synorogenic foreland rifts and transtensional basins: A review of Andean imprints on the evolution of the San Jorge Gulf, Salta Group and Taubaté Basins. J. S. Am. Earth Sci. 64, 288-306.

Gianni, G.M., Echaurren, A., Folguera, A., Likerman, J., Encinas, A., García, H.P.A., Dal molin, C.,Valencia, V.A., 2017. Cenozoic intraplate tectonics in Central Patagonia: Record of main Andean phases in a weak upper plate. Tectonophysics, 721, 151-166.

González Díaz, E., 1979. Estratigrafía del área de la Cordillera Patagónica entre los paralelos 40º 30' y 41º 00' de latitud sur (provincia del Neuquén). VII Congreso Geológico Argentino, Neuquén, Actas 1: 525-537

González Díaz, E., 1982. Zonación cronológica del plutonismo en los Andes Patagónicos Septentrionales entre los 40º y 42º sur: la migración de los ciclos intrusivos. Acta Geológica Lilloana 16 (1): 5-22

Guillot, M.G., Escayola, M., Acevedo, R., 2011. Calc-alkaline rear-arc magmatism in the Fuegian Andes: Implications for the mid-cretaceous tectonomagmatic evolution of southernmost South America. J. S. Am. Earth Sci. 31(1), 1-16

Grove, T., Till, C., Lev, E., Chatterjee, N., Medard, E., 2009. Kinematic variables and water transport control the formation and location of arc volcanoes. Nature, 459, 694–697 (2009); erratum 460, 1044 (2009)

Grove, T.L., Till, C.B., Lev, E., Chatterjee, N., Medard, E., 2010. Global systematics of arc volcano position, Grove et al. reply. Nature, 468:E7–8

Groeber, P., 1946. Observaciones geológicas a lo largo del meridiano 70º. 2. Hojas Sosneado y Maipo. Rev. Soc. Geol. Arg. 2 (2), 141–176

Gulisano, C.A., Gutiérrez Pleimling, A.R., 1994. The Jurassic of the Neuquén Basin. Field Guide. Asoc, Geol, Arg, Series E, 111

Gutscher, M.A., Spakman, W., Bijwaard, H., Engdahl, E.R., 2000. Geodynamic of flat subduction: seismicity and tomographic constraints from the Andean margin. Tectonics, 19, 814–833

Guivel, C., Lagabrielle, Y., Bourgois, J., Martin, H., Arnaud, N., Fourcade, S., cotton, J., Maury, R.C., 2003. Very shallow melting of oceanic crust during spreading ridge subduction: origin of near-trench Quaternary volcanism at the Chile Triple Junction. J. Geoph. Res. 108, 2345 doi:10.1029/2002JB002119.

Hager, B.H., O'Connell, R.J., 1979. Kinematic models of large-scale flow in the Earth's man-tle. J. Geophys. Res., Solid Earth 84 (B3), 1031–1048.

Hager, B.H., 1984. Subducted slabs and the geoid: constraints on mantle rheology and flow. J. Geophys. Res. 89 (B7), 6003–6015.

Hager, B.H., O'Connell, R.J., 1981. A simple global model of plate dynamics and man-tle convection. J. Geophys. Res., Solid Earth8 (B6), 4843–4867.

Hallam, A., Cohen, J., 1989. The case for sea-level change as a domi- nant causal factor in mass extinction of marine invertebrates [and discussion]. Phil. Trans. Royal Soc. B. (Biologi-cal sciences) London, 325, 437-455.

Haller, M., Lapido, O., 1980. El Mesozoico de la Cordillera Patagónica Central. Revista de la Asociación Geológica Argentina. Rev. Asoc. Geol. Argent. 35, 230–247.

Haller, M.J., Lech, R.R., Meister, C.M., Martínez, O., Poma, S., Viera, R.L.M., 2010. Des-cripción geológica de la Hoja Geológica 4373-IV/III, Trevelin, Provincia de Chubut. Serv. Geol. Min. Arg., Instituto de Geología y Recursos Minerales, Boletín 322, 55

Haq, B., Hardenbol, J., Vail, P., 1987. Chronology of fluctuating sea levels since the Triassic. Science, 235, 1156-1167.

Halpern, M., Stipanicic, P., Toubes, R., 1975. Geocronología (Rb/Sr) en los Andes Australes Argentinos. Rev. Asoc. Geol. Arg. 30 (2), 180-192

Haschke, M.R., Siebel, W., Günther, A., Scheuber, E., 2002. Repeated crustal thickening and recycling during the Andean orogeny in north Chile (21°–26°S). J. Geoph. Res., 107, p. 1–18, doi: 10.1029/2001JB000328.

Hay, W.W., 2008. Evolving ideas about the Cretaceous climate and ocean circulation. Cret. Res. 29 725–753.

Heller, P.L., Liu, L. 2016. Dynamic topography and vertical motion of the US Rocky Mountain region prior to and during the Laramide orogeny. GSA Bulletin 128(5-6), 973-988.

Homovc, J., Conforto, G., Lafourcade, P., Chelotti, L., 1995. Fold Belt in the San Jorge Basin, Argentina: an Example of Tectonic Inversion. In: P. Buchanan, J. y Buchanan (eds), Basin Inversion, Geol. Soc. London Special Publication, pp 235–248

Homovc, J.F., Constantini, L., 2001. Hydrocarbon exploration potential within intraplate shear-related depocenters: Deseado and San Julián basins, southern Argentina. Am. Assoc. Pet. Geol. Bull. 85, 1795–1816.

Horton, B.K., Hampton, B.A., Waanders, G., 2001. Paleogene synorogenic sedimentation in the Altiplano plateau and implications for initial mountain building in the central Andes: Geol. Soc. Am. Bull. 113, 1387–1400, doi: 10 .1130 /0016 -7606 (2001)113 <1387: PSSITA >2 .0 .CO;2.

Horton, B.K., Fuentes, F., 2016. Sedimentary record of plate coupling and decoupling during growth of the Andes. Geology, 44(8), 647-650

Horton, B.K., 2017. Sedimentary record of Andean mountain building. Earth-Sci Rev.

Horton, B.K., 2018. Tectonic regimes of the central and southern Andes: Responses to variations in plate coupling during subduction. Tectonics. In press

Hoorn, C., Wesselingh, F. P., Ter Steege, H., Bermudez, M. A., Mora, A., Sevink, J., ... & Jaramillo, C., 2010. Amazonia through time: Andean uplift, climate change, landscape evolution, and biodiversity. Science, 330(6006), 927-931.

Hu, J., Liu, L., Hermosillo, A., Zhou, Q., 2016. Simulation of late Cenozoic South American flat-slab subduction using geodynamic models with data assimilation. Earth Planet. Sci. Lett. 438, 1-13.

Humphreys, E.D., 1995. Post-Laramide removal of the Farallon slab, western United States. Geology, 23(11), 987-990.

Husson, L., Conrad, C.P., Faccenna, C., 2008. Tethyan closure, Andean orogeny, and westward drift of the Pacific Basin. Earth Planet. Sci. Lett. 271 (1), 303–310

Iannelli, S.B., Litvak, V.D., Fernandez Paz, L., Folguera, A., Ramos, M.E., Ramos, V.A., 2017. Evolution of Eocene to Oligocene arc-related volcanism in the north patagonian Andes (3941S), prior to the break-up of the Farallon plate. Tectonophysics, 696-697, 70-87. https://doi.org/10.1016/j.tecto.2016.12.024

Iannelli, S.B., Fennell, L., Litvak, V.D., Fernández Paz, L., Encinas, A., Folguera, A., 2018. Geochemical and tectonic evolution of Late Cretaceous to early Paleocene magmatism along the Southern Central Andes (35-36ºS). J. South Am. Earth Sci. doi: 10.1016/j.jsames.2017.12.008.

Iannizzotto, N.F., Folguera, A., Leal, P.R., 2004. Control tectónico de las secuencias volcaniclásticas neocomianas y paleogeografía en la zona del Lago La Plata (45ºS). Sector interno de la faja plegada y corrida de los lagos La Plata y Fontana. Rev. Asoc. Geol. Arg. 59, 655–6708

IIG/MMAJ/JICA, 1978. Informe de reconocimiento geológico del área Coihueco-Ñuble-Lonquimay (Malleco), Central Sur de Chile, fase III (inédito). Instituto de Investigaciones Geológicas. Vol. 1: 335 p. Santiago.

Jaimes, E., de Freitas, M., 2006. An Albian–Cenomanian unconformity in the northern Andes: evidence and tectonic significance. J. S. Am. Earth Sci. 21, 466–492

Jaillard, E., Bengtson, P., Dhondt, A.V., 2005. Late Cretaceous marine transgressions in Ecuador and northern Peru: a refined stratigraphic framework. J. S. Am. Earth Sci. 19, 307–323

Jones, C.H., Farmer, G.L., Sageman, B., Zhong, S.J., 2011. Hydrodynamic mechanism for the Laramide orogeny. Geospher,e 7, 183–201. http://dx.doi.org/10.1130/GES00575.1.

Jordan, T., Burns, W., Veiga, R., Pángaro, F., Copeland, P., Kelley, S., Mpodozis, C. 2001. Extension and basin formation in the Southern Andes caused by increased convergence rate: a Mid-Cenozoic trigger for the Andes. Tectonics, 20 (3), 308-324

Karlstrom, L., Lee, C.T., Manga, M., 2014. The role of magmatically driven lithospheric thickening on arc front migration. Geoch. Geophy. Geosyst. 15(6), 2655-2675.

Kay, S.M., Mpodozis, C., Coira, B., 1999. Neogene magmatism, tectonism, and mineral deposits of the Central Andes (22°S to 33°S). In: Skinner, B. et al. (eds) Geology and Mineral Deposits of Central Andes. Soc. Ec. Geol., Special Publication 7:27–59

Kay, S.M., Godoy, E., Kurtz, A., 2005. Episodic arc migration, crustal thickening, subduction erosion, and magmatism in the south-central Andes: Geological Society of America Bulletin, v. 117, p. 67–88, doi: 10.1130/B25431.1.

Kay, S.M., Ardolino, A.A., Gorring, M.L., Ramos, V.A., 2006. The Somuncura large igneous province in Patagonia: interaction of a transient mantle thermal anomaly with a subducting slab. J. Petrol. 48, 43–77. http://dx.doi.org/10.1093/petrology/egl053.

Kay, S.M., Copeland. P., 2006. Early to middle Miocene backarc magmas of the Neuquén Basin: geochemical consequences of slab shallowing and the westward drift of South America. In: Kay, S.M., Ramos, V.A. (Eds.), Evolution of an Andean Margin: A Tectonic and Magmatic View from the Andes to the Neuquén Basin (35°-39°S lat.). Geol. Soc. Am. Special Paper 407:185-213

Kozlowski, E., Manceda, R., Ramos, V.A., 1993. Estructura. In: Ramos, VA (ed.) Geología y Recursos Naturales de Mendoza, Relatorio del XII Congreso Geológico Argentino y II Congreso de Exploración de Hidrocarburos 235-256

Mamani, M., Wörner, G., Sempere, T., 2010. Geochemical variations in igneous rocks of the Central Andean orocline (13 S to 18 S): Tracing crustal thickening and magma generation through time and space. Geol. Soc. Am. Bull.,122(1-2), 162-182.

Manceda, R., Figueroa, D., 1995. Inversion of the Mesozoic Neuquén rift in the Malargüe fold-thrust belt, Mendoza, Argentina. In: Tankard, A.J., Suarez, R.S., Welsink, H.J. (Eds.), Petroleum basins of South America, Am. Assoc. Petrol. Geol. Mem. 62, 369-382

Maloney, K.T., Clarke GL, Klepeis KA, Quevedo L (2013) The Late Jurassic to present evolution of the Andean margin: Drivers and the geological record, Tectonics 32. doi:10.1002/tect.20067

Martin-Gombojav, N., Winkler, W., 2008. Recycling of Proterozoic crust in the Andean Amazon foreland of Ecuador: implications for orogenic development of the Northern Andes. Terra Nova, 20:22–31

Megard, F., 1984. The Andean orogenic period and its major structures in central and northern Peru: Journal of the Geological Society of London, 141, 893–900, doi:10.1144/gsjgs.141.5.0893.

Mescua, J.F., Giambiagi, L.B., Ramos, V.A., 2013. Late Cretaceous Uplift in the Malargüe fold-and-thrust belt (35ºS), southern Central Andes of Argentina and Chile. And. Geol. 40 (1):102-116

Micucci, E.M., Continanzia, J., Manceda, R., Gavarrino, A.S., 2011. Cuenca de San Julián: Síntesis del conocimiento exploratorio – visión actual. In: Kozlowski, E., Legarreta, L., Boll, A., Marshall, P.A. (Eds), Simposio Cuencas Argentinas Visión Actual: VIII Congreso de Exploración y Desarrollo de Hidrocarburos, pp 17–46

Miller, K., Kominz, M., Browning, J., Wright, J., Mountain, G., Katz, M., Sugarman, P., Cramer, B., Christie-black, N., Pekar, S., 2005. The Phanerozoic record of global sea-level change. Science, 310, 1293-1298.

Mitrovica, J. X., Beaumont, C., Jarvis, G.T., 1989. Tilting of the continental interior by the dynamical effects of subduction. Tectonics, 8 (5), 1079–1094.

Molnar, P., Freedman, D., Shih, J.S.F., 1979. Lengths of intermediate and deep seismic zones and temperatures in downgoing slabs of lithosphere. Geophys. J. Roy. Astronom. Soc. 56, 41–

54.

Moreno, H., Lara, L., 2008. Geología del área Pucón-Curarrehue, regiones de La Araucanía y de Los Ríos, Escala 1:100.000. SERNAGEOMIN, Carta Geológica de Chile, Serie Geología Básica (Nº 115): 36 p., 1 mapa pleg.col, Santiago.

Mpodozis, C., Arriagada, C., Basso, M., Roperch, P., Cobbold, P., Reich, M., 2005. Late Mesozoic to Paleogene stratigraphy of the Salar de Atacama Basin, Antofagasta, Northern Chile: Implications for the tectonic evolution of the Central Andes. Tectonophysics, 399(1-4), 125-154

Munizaga, F., Hervé, F., Drake, R., Pankhurst, R.J., Brook, M., Snelling, N., 1988. Geochronology of the Lake region of south-central Chile (39°-42°S): preliminary results. J. South Am. Earth Sci. 1(3), 309-316

Muñoz, J., Troncoso, R., Duhart, P., Crignola, P., Farmer, L., Stern, C.R., 2000. The relation of the mid-Tertiary coastal magmatic belt in south-central Chile to the late Oligocene increase in plate convergence rate. Rev. Geol. Chile 27. http://dx.doi.org/ 10.4067/S0716-02082000000200003.

Mulch, A., Uba, C. E., Strecker, M. R., Schoenberg, R., Chamberlain, C. P., 2010. Late Miocene climate variability and surface elevation in the central Andes. Earth Planet. Sci. Let. 290(1), 173-182.

Müller, R.D., Seton, M., Zahirovic, S., Williams, S.E., Matthews, K.J., Wright, N.M., Shephard, G.E., Maloney, K.T., Barnett-Moore, N., Hosseinpour, M., Bower, D.J., 2016. Ocean basin evolution and global-scale plate reorganization events since Pangea breakup. Ann. Rev. Earth Planet. Sci. 44, 107-138.

Navarrete, C. R., Gianni, G. M., Folguera, A., 2015. Tectonic inversion events in the western San Jorge Gulf Basin from seismic, borehole and field data, J. South Am. Earth Sci. 64, 486-497

Nullo, F., Combina, A., 2011. Patagonian continental deposits (Cretaceous-Tertiary). Biological J. Linn. Soc. 103(2), 289-304

Lagorio, S., Montenegro, G., Massaferro, Vattuone, M.E., 1998. Edad y geoquímica de las ignimbritas de Aluminé, provincia del Neuquén, Argentina. In: 10° Congreso Latinoamericano de Geología Económica (Buenos Aires), Actas 2:231-325

Lara, L., Moreno, H., 2004. Geología del área Liquiñe-Neltume, regiones de La Araucanía y de Los Lagos, Escala 1:100.000. Servicio Nacional de Geología y Minería, Carta Geológica de Chile, Serie Geología Básica (Nº 83): 23 p., 1 mapa pleg. col, Santiago.

Leanza, H., 2009. Las principales discordancias del Mesozoico de la Cuenca Neuquina según observaciones de superficie. Rev. del Mus. Argent. Ciencias Nat. 11(2), 145-184

Legarreta, L., Gulisano, C., 1989. Análisis estratigráfico secuencial de la Cuenca Neuquina (Triásico superior-Terciario inferior). In: Chebli, G., Spalletti, L., (Eds.), Cuencas Sedimentarias Argentinas, Correlación Geológica, serie 6:221–243

Lesta, P., Ferello, R., Chebli, G., 1980. Chubut extraandino. In: Turner JC (ed), II Simposio de Geología Regional Argentina, Academia Nacional de Ciencias, Córdoba, pp 1307–1387

Li, Z.X., Li, X.H., 2007. Formation of the 1300-km-wide intracontinental orogen and postorogenic magmatic province in Mesozoic South China: a flat-slab subduction model. Geology, 35(2), 179-182.

Linares, E., González, R.R., 1990. Catálogo de edades radimétricas de la República Argentina 1957-1987. As. Geol. Arg., Publicaciones Especiales, Serie B, Didáctica y Complementaria 19, p. 1-628

Lithgow-Bertelloni, C., Gurnis, M., 1997. Cenozoic subsidence and uplift of continents from time-varying dynamic topography. Geology, 25 (8), 735–738.

Liu, L., Spasojević, S., Gurnis, M., 2008 Reconstructing Farallon plate subduction beneath North America back to the Late Cretaceous. Science, 322(5903), 934-938.

Liu, L., Gurnis, M., Seton, M., Saleeby, J., Müller, R.D., Jackson, J.M., 2010. The role of oceanic plateau subduction in the Laramide orogeny. Nat. Geosc. 3(5), 353.

Lizuaín, A., 1979. La edad de las sedimentitas del cerro Plataforma, provincia del Chubut. Rev. Asoc. Geol. Arg., 34 (1), 69-72

Lizuaín, A., 1980. Las formaciones Suprapaleozoicas y Jurásicas de laCordillera Patagónica. Provincias de Río Negro y Chubut. Rev. Asoc. Geol. Arg. 35(2), 174-186

Lizuaín, A., 1981. Características y edad del plutonismo en los alrededores del lago Puelo. Provincia del Chubut. VIII Congreso Geológico Argentino, Neuquén, Actas 3: 607-616

Lizuaín, A., 1987. El vulcanismo cretácico de la Cordillera Patagónica entre los lagos Puelo y Cholila, provincia del Chubut. X Congreso Geológico Argentino, San Miguel de Tucumán, Actas 4:213-216

Liu, S., Nummedal, D., Liu, L., 2011. Migration of dynamic subsidence across the Late Cretaceous United States Western Interior Basin in response to Farallon plate subduction. Geology, 39 (6), 555–558.

Llambías, E.J., Rapela, C.W., 1989. Las vulcanitas de Colipilli, Neuquén (37ºS) y su relación con otras unidades paleógenas de la cordillera. As. Geol. Arg. XLIV (1-4):224-236

LLambías, E.J., Aragón, E., 2011. Volcanismo Paleógeno. In: Leanza, H.A., Arregui, O., Carbone, O., Danieli, J.C., Vallés, J.M. (Eds.), Geología y recursos naturales de la Provincia del Neuquén Relatorio del XVIII Congreso Geológico Argentino 265–274

López de Luchi, M.G., Spikermann, J.P., Strelin, J.A., Morelli, J., 1992. Geología y petrología de los plutones de la Tapera de Burgos, Arroyo el Rápido y Cerro Caquel, Departamento Languineo, Provincia del Chubut. Rev. Asoc. Geol. Argent. 47, 87–98

Olivero, E.B., Medina, F.A., 1994. Sedimentología de la Formación Lefipán (Cretácico-Terciario) en el valle medio del Río Chubut. Rev. Asoc. Geol. Arg., 48, 105-106

Oncken, O., Hindle, D., Kley, J., Elger, K., Victor, P., Schemmann, K., 2006. Deformation of the Central Andean upper plate system—Facts, fiction, and constraints for plateau models. In: Oncken, O., Chong, G., Franz, G., Giese, P., Götze, H.J., Ramos, V.A., Strecker, M.R., Wigger, P. (Eds.), The Andes, Springer Berlin Heidelberg 22:3-27

Olson, P., Nam, S., 1986 Formation of seafloor swells by mantle plumes. J. Geophys. Res. 91 (B7), 7181–7191.

Orts, D.L, Folguera, A., Giménez, M., Ramos, V.A., 2012a. Variable structural controls through time in the Southern Central Andes (~36ºS). And. Geol. 39 (2), 220-241

Orts, D.L., Folguera, A., Encinas, A., Ramos, M., Tobal, J., Ramos, V.A. 2012b. Tectonic development of the North Patagonian Andes and their related Miocene foreland basin (41°30′–43° S). Tectonics, 31, 1–24

Pankhurst, R.J., Hervé, F., Rojas, L., Cembrano, J., 1992. Magmatism and tectonics in continental Chiloé, Chile (42–42 30′ S). Tectonophysics, 205, 283–294

Pankhurst, R.J., Hervé, F., 1994. Granitoid age distribution and emplacement control in the North Patagonian batholith in Aysen (44°-47°S). VII Congreso Geológico Chileno, Concepción, Actas 2: 1409-1413

Pankhurst, R.J., Weaver, S.D., Hervé, F., Larrondo, P., 1999. Mesozoic–Cenozoic evolution of the North Patagonian batholith in Aysen, southern Chile. J. Geol. Soc. 156, 673–69

Pankhurst, R.J., Hervé, F., Fanning, M., Suárez, M., 2003. Coeval plutonic and volcanic activity in the Patagonian Andes: the Patagonian Batholith and the Ibáñez and Divisadero For-

mations, Aisén, southern Chile. In: X Congreso Geológico Chileno (ed Campos E). Electronic files

Pankhurst, R.J., Rapela, C., Fanning, C., Márquez, M., 2006. Gondwanide continental collision and the origin of Patagonia. Earth Sci. Rev. 76, 235–257

Parada, M.A., Lahsen, A., Palacios, C., 2001. Ages and geochemistry of Mesozoic-Eocene back-arc volcanic rocks in the Aysén region of the Patagonian9 Andes. Rev. Geol. Chile 28, 25-46

Pérez-Gussinyé, M., Swain, C.J., Kirby, J.F., Lowry, A.R., 2009. Spatial variations of the effective elastic thickness, Te, using multitaper spectral estimation and wavelet methods: examples from synthetic data and application to South America. Geoch. Geoph. Geosyst. 10(4).

Perez Loinaze, V.S., Vera, E.I., Passalia, M.G., Llorens, M., Friedman, R., Limarino, C.O., Césari, S.N., 2013. High-precision U–Pb zircon age from the Anfiteatro de Ticó Formation: Implications for the timing of the early angiosperm diversification in Patagonia. J, South Am. Earth Sci. 48, 97–105

Pesce, A., 1979. Estratigrafía de la Cordillera Patagónica entre los 43º 30´ y 44º de latitud sur y sus áreas mineralizadas. VII Congreso Geológico Argentino, Buenos Aires 1: 257-270

Peroni, G.O., Hegedus, A.G., Cerdan, J., Legarreta, L., Uliana, M.A., 1995. Hydrocarbon Accumulation in an Inverted Segment of the Andean Foreland : San Bernardo Belt, Central Patagonia. In: Tankard, A.J., Suárez, R., Welsink, H.J. (Eds.), Petroleum Basins of South America, pp 403–419

Poulsen, C. J., Ehlers, T. A., Insel, N., 2010. Onset of convective rainfall during gradual late Miocene rise of the central Andes. Science, 328(5977), 490-493.

Rabassa, J., 1978. Estratigrafía de la región de Pilcaniyeu Comallo, Provincia de RíoNegro. VII Congreso Geológico Argentino, Neuquén, Actas 1: 731-746

Raimondo, T., Hand. M., Collins, W.J., 2014. Compressional intracontinental orogens: Ancient and modern perspectives. Earth-Science Rev. 130, 128–153, 760 doi:10.1016/j.earscirev.2013.11.009.

Ramos, V.A., 1981a. Descripción geológica de la Hoja 33c Los Chihuidos Norte, Provincia del Neuquén. Servicio Geológico Nacional, Boletín 182, 1–103 Buenos Aires.

Ramos, V.A., 1981b. Descripción geológica de la hoja 47 ab Lago Fontana, Provincia de Chubut. Servicio Geológico Nacional. Bol., Buenos Aires 183,130

Ramos, V.A., 1982 Geología de la región del lago Cardiel, provincia de Santa Cruz. Rev. Asoc. Geol. Arg. 37, 23-49

Ramos, V.A., Cortés, J.M., 1984. Estructura e interpretación tectónica, Geol. y Recur. Nat. la Prov. Río Negro, 1, 12

Ramos, V.A., 1999. Rasgos estructurales del territorio argentino. Geología Argentina (Caminos, R.; editor). Instituto de Geología y recursos Minerales, Anales, 29(24), 715-784.

Ramos, V.A., Folguera, A., 2005. Tectonic evolution of the Andes of Neuquén: constraints derived from the magmatic arc and foreland deformation. In: Veiga, G.D., Spalletti, L.A., Howell, J.A., Schwarz, E. (Eds.), The Neuquén Basin, Argentina: A case Study in Sequence Stratigraphy and Basin Dynamics Geol. Soc. Lond., Special Publications, 252:15-35

Ranalli, J.N., Peroni, G.O., Boggetti, D.A., Manoni, R., 2011. Cuenca Cañadón Asfalto. Modelo tectosedimentario. In: Kozlowski, E., Legarreta, L., Boll, A., Marshall, P.A. (Eds), Simposio Cuencas Argentinas Visión Actual: VIII Congreso de Exploración y Desarrollo de Hidrocarburos pp 185–216

Rapela, C.W., Spalletti, L., Merodio, J.C., 1983. Evolución magmática y geotectónica de la Serie Andesitica andina (Paleoceno-Eoceno) en la cordillera norpatagónica. Rev. Asoc. Geol. Arg. 38 (3-4), 469-484

Rapela, C., Munizaga, F., Dalla Salda, L., Hervé, F., Parada, M., Cingolani, C., 1987. Nuevas edades K-Ar de los granitoides del sector nororiental de los Andes Patagónicos. X Congreso Geológico Argentino, Tucumán, Actas 4, 18-20

Rapela, C.W., Kay, S.M., 1988. Late Paleozoic to recent magmatic evolution of northern Patagonia, Episodes, 11, 175–182

Rapela, C.W., Pankhurst, R.J., Fanning, C.M., Hervé, F., 2005. Pacific subduction coeval with the Karoo mantle plume: the Early Jurasssic Subcordilleran belt of northwestern Patagonia. Geol. Soc. Lond., Special Publications 246(1), 217-239

Reimer, W., Miller, H., Mehl, H., 1996. Mesozoic and Cenozoic palaeo-stress fields of the South Patagonian Massif deduced from structural and remote sensing data. Geol. Soc. Lond., Special Publications 108(1), 73-85

Rojas Vera, E., Mescua, J., Folguera, A., Becker, T.P., Sagripanti, L., Fennell, L., Orts, D., Ramos, V.A., 2015. Evolution of the Chos Malal and Agrio fold-thrust belts, Andes of Neuquén: Insights from structural analysis and apatite fission track dating. J. South Am. Earth Sci. 64, 418-433.

Rohrmann, A., Strecker, M.R., Bookhagen, B., Mulch, A., Sachse, D., Pingel, H., Alonso, R., Schildgen, T., Montero, C., 2014. Can stable isotopes ride out the storms? The role of convection for water isotopes in models, records, and paleoaltimetry studies in the central Andes. Earth Planet. Sci. Let., 407, 187-195.

Sagripanti, L., Bottesi, G., Naipauer, M., Folguera, A., Ramos, V.A., 2011. U/Pb ages on detrital zircons in the southern central Andes Neogene foreland (36º-37ºS): Constraints on Andean exhumation, J. South Am. Earth Sci. 32 (4), 555-566.

Savignano, E., Mazzoli, S., Arce, M., Franchini, M., Gautheron, C., Paolini, M., Zattin, M. (2016) (Un) Coupled thrust belt-foreland deformation in the northern Patagonian Andes: new insights from the Esquel-Gastre sector (41° 30'–43° S). Tectonics.

Soechting, W., 2001. Tectonic control of epithermal gold mineralization in the Cordon de Esquel, Chubut. Argentina. Minera El Desquite S.A. Esquel. Unpublished report.

Spalletti, L.A., Franzese, J.R., 1996. Mesozoic palaeogeography of southern South America. Third International Symposium on Andean Geodymanics, Paris, 497–500.

Sánchez, M.L., Asurmendi, E., 2014. Modelo de depósito de la Formación Cerro Lisandro: lóbulos de desembocadura y deltas de tipo Gilbert. Cretácico superior, región central de cuenca Neuquina, Argentina. Rev. Mex. Cien. Geol. 31 (2), 141-162

Scasso, R.A., Aberhan, M., Ruiz, L.,Weidemeyer, S., Medina, F.A., Kiessling, W., 2012. Integrated bio-and lithofacies analysis of coarse-grained, tide-dominated deltaic environments across the Cretaceous/Paleogene boundary in Patagonia, Argentina. Cretac. Res. 36, 37–57

SEGEMAR-JICA- MMAJ-JMEC, 1999-2000- 2001. Regional Survey for Mineral Ressources in the Southern Andes Area. Convenio de Cooperación Técnica entre el SEGEMAR, Counterpart for República Argentina y JICA, MMAJ y JMEC of Japan. SEGEMAR. Trabajo inédito. Buenos Aires.

Sepúlveda, E.G., Viera, R.M., 1980. Geología y área de alteración en el cerro Colorado y alrededores,Chubut noroccidental. Rev. Asoc. Geol. Arg. 35 (2), 195-202

Sempere, T., 1995. Phanerozoic evolution of Bolivia and adjacent regions. In: Tankard, A.J., et al. (Ed.), Petroleum Basins of South America: Am Assoc Petr Geol, Memoir 62:207–230

Silva Nieto, D., 2005. Hoja Geológica 4369-III, Paso de Indios, provincia del Chubut Vol. 265. Instituto Geología y Recursos Minerales, Servicio Geológico Minero Argentino, Boletín, p. 72

Silvestro, J., Atencio, M., 2009. La cuenca Cenozoica del Río Grande y Palauco: Edad, evolución y control estructural, faja plegada de Malargüe (36ºS). Rev. Asoc. Geol. Arg. 65 (1), 154-169

Silvestro, J., Kraemer, P., Achilli, F., Brinkworth, W., 2005 Evolución de las cuencas sinorogéncias de la Cordillera Principal entre 35º - 36º S, Malargüe. Rev. Asoc. Geol. Arg. 60 (4), 627-643

Soler, P., Bonhomme, M.G., 1990. Relation of Magmatic Activity to Plate Dynamics ìn Central Peru from Late Cretaceous to Present. In Plutonism from Antarctica to Alaska; Special Paper 241; Kay, S.M., Rapela, C.W. et al. (Eds.) Geol. Soc. Ame.: Boulder, CO, USA, pp. 173–192

Spagnuolo, M.G., Folguera, A., Litvak, V., Rojas Vera, E.A., Ramos, V.A., 2012. Late Cretaceous arc rocks in the Andean retroarc region at 36,5ºS: Evidence supporting a Late Cretaceous slab shallowing. J. S. Am. Earth Sci. 38, 44-56

Suárez, M., Emparán, C, Muñoz, J., 1986. Geología de la parte oriental de la Hoja Curacautín, IX Región (Inédito). Servicio Nacional de Geología y Minería, 119 p.

Suárez, M., De La Cruz, R., Bell, M., 1996. Estratigrafía de la región de Coyhaique (45º–46º latitud S); Cordillera Patagónica, Chile. In: Ramos, V.A. et al (Eds.), XIII Congreso Geológico Argentino and III Congreso de Exploración de Hidrocarburos, pp 575–90. Buenos Aires.

Suárez, M., De la Cruz, R., 2001. Jurassic to Miocene K–Ar dates from eastern central Patagonian Cordillera plutons, Chile (45–48 S). Geol. Mag. 138, 53-66

Suárez, M., De La Cruz, R., Bell, M.C., 2007. Geología del Area Ñireguao–Baño Nuevo, Región Aisén del General Carlos Ibáñez del Campo. Servicio Nacional de Geología y Minería, Carta Geológica de Chile, Serie Geología Básica 108: 1–56. Santiago

Suárez, M., Márquez, M., 2007. A Toarcian retro-arc basin of Central Patagonia (Chubut), Argentina: Middle Jurassic closure,arc migration and tectonic setting. Rev. Geol. Chile 34(1), doi:10.4067/S0716-02082007000100004.

Suárez, M., De La Cruz, R., Bell, M., Demant, A., 2009a. Cretaceous slab segmentation in southwestern Gondwana. Geol. Mag. 147:193-205

Suárez, M., Márquez, M., De La Cruz, R., Fanning, M., 2009b. Aptian-Albian subaerial volcanic rocks in central Patagonia : Divisadero and Chubut Groups. In: XII Congreso Geológico Chileno, pp 1–4

Suárez, M., Márquez, M., De La Cruz, R., Navarrete, C., Fanning, M., 2014. Cenomanian-? Early Turonian Minimum Age of the Chubut Group, Argentina: SHRIMP U-Pb geochronology. J. South Am. Earth Sci. 50, 64-74

Tapia, F., 2015. Evolución tectónica y configuración actual de los Andes Centrales del sur 1449 (34° 45'-35° 30'S), Ph.D. thesis, Universidad de Chile, Santiago, Chile.

Tassara, A., Götze, H.J., Schmidt, S., Hackney, R., 2006. Threeötze HJ, Sch density model of the Nazca plate and the Andean continental margin. J. Geoph. Res.: Solid Earth, 111(B9).

Tatsumi, T., Eggins, S., 1995. Subduction Zone Magmatism. Wiley-Blackwell.

Toubes, R.O., Spikerman, J.P., 1973. Algunas edades K/Ar y Rb/Sr de plutonitas de la Cordillera Patagónica entre los paralelos 40º y 44º de latitud sur. Rev. Asoc. Geol. Arg. 28(4), 382-39.

Tunik, M.A., Vietto, M.E., Sciutto, J.C., 2004. Procedencia de areniscas del Grupo Chubut en el área central de la Sierra de San Bernardo. Análisis preliminar. Rev. Asoc. Geol. Arg. 59, 601–606

Tunik, M., Folguera, A., Naipauer, M., Pimentel, M., Ramos, V.A., 2010. Early uplift and orogenic deformation in the Neuquén Basin: Constraints on the Andean uplift from U-Pb and Hf isotopic data of detrital zircons. Tectonophysics, 489, 258-273

Turner, J.C., 1982. Descripción geológica de la Hoja 44c, Tecka, Provincia del Chubut. Servicio Geológico Nacional, Boletín Vol. 180, pp. 1–92

Turienzo, M., Dimieri, L., Friscale, C., Araujo, V., Sánchez, N., 2012. Cenozoic structural evolution of the Argentinean Andes at 34º40'S: A close relationship between thick and thin-skinned deformation. And. Geol. 39 (2):317-357

Uliana, M.A., Biddle, K.T., 1988. Mesozoic–Cenozoic paleogeographic and geodynamic evolution of southern South America. Rev. Bra. Geoc. 18, 172–190

Uliana, M.A., Biddle, K.T., Cerdan, J., 1989. Mesozoic extension and the formation of Argentine sedimentary basins. In: Tankard, A.J., Balkwill, H.R. (Eds.) Extensional Tectonics and Stratigraphy of the North Atlantic Margin pp 599-613

van Hunen, J., van den Berg, A.P., Vlaar, N.J., 2000. A thermo-mechanical model of horizontal subduction below an overriding plate. Earth Planet. Sci. Lett.182 (2), 157–169.

van Hunen, J., van den Berg, A.P., Vlaar, N.J., 2002. On the role of subducting oceanic plateaus in the development of shallow flat subduction. Tectonophysics, 352, 317–333. http://dx.doi.org/10.1016/S0040-1951(02)00263-9.

Varela, R., Basei, M., Cingolani, C., Siga, Jr. O., Passarelli, C., 2005. El basamento cristalino de los Andes norpatagónicos en Argentina: geocronología e interpretación tectónica. Rev. Geol. Chile 32 (2), 167-187

Vattuone, M.E., Latorre, C.O., 2004. Edades K/Ar al este del cerro Nahuel Pan, Chubut.Implicancias en la correlacion del Grupo Divisadero y del Choiyoi en el área. Rev Asoc. Geol. Arg. 59(3), 510-513.

Vérard, C., Hochard, C., Baumgartner, P.O., Stampfli, G.M., Liu, M., 2015. 3D palaeogeographic reconstructions of the Phanerozoic versus sea-level and Sr-ratio variations. J. Palaeog. 4(1), 64-84.

Vergani, G.D., Tankard, A.J., Belotti, H.J., Welsink, H.J., 1995. Tectonic evolution and paleogeography of the Neuquén Basin, Argentina. In: Tankard, A.J., Suárez Soruco, R., Welsink, H.J. (Eds.), Petroleum Basins of South America. Am Assoc Petrol Geol, Memoirs, 62, pp. 383–402

von Huene, R., Scholl, D.W., 1991. Observations at convergent margins concerning sediment subduction, subduction erosion, and the growth of continental crust. Rev. Geophys. 29, 279–316, doi: 10.1029/91RG00969.

Weaver, C. 1927. The Roca Formation in Argentina. Am. J. Sci. 13, 417–434

Wilson, T.J., 1991. Transition from Back-Arc to Foreland Basin Development in the Southernmost Andes – Stratigraphic Record from the Ultima-Esperanza-District, Chile. Geol. Soc. Am. Bull., 103, 98–111.

Zaffarana, C., Lagorio, S., Busteros, A., Silva Nieto, D., Giacosa, R., Ruiz González, V., Boltshauser, B., Somoza, R., Haller, M., 2017. Hallazgo de magmatismo Cretácico Tardío en la zona de Gastre, Macizo Norpatagónico. In: XX Congreso Geológico Argentino. Electronic book. Tucumán. http://congresogeologico.org.ar/

Zamora Valcarce, G., Zapata, T., Del Pino, D., Ansa, A., 2006. Structural evolution and magmatic characteristics of the Agrio Fol. and thrust belt. In: Kay, S.M., Ramos, V.A. (Eds.), Evolution of an Andean Margin: A Tectonic and Magmatic View from the Andes to the Neuquén Basin (35°-39° lat). Geol. Soc. Am., Special Paper 407, pp. 125-145

Zamora Valcarce, G., Rapalini, A.E., Spagnuolo, C.M., 2007. Reactivación de estructuras cretácicas durante la deformación miocena, faja plegada del Agrio, Neuquén. Rev. Asoc. Geol. Arg. 62 (2), 299-308

Zamora Valcarce, G., Zapata, T., Ramos, V.A., Rodríguez, F., Bernardo, L.M., 2009. Evolución tectónica del frente andino en Neuquén. Rev. Asoc. Geol. Arg. 65(1), 192-203

Zhong, S., Gurnis, M., 1994. Controls on trench topography from dynamic models of subducted slabs. J. Geoph. Res. 99, NO. B8, PAGES 15,683-15, 695.